The Thesis Committee for Shubham Agrawal
Certifies that this is the approved version of the following thesis:

Decision Analysis and Risk Management: Application to Climate Change and Risk Detection

APPROVED BY
SUPERVISING COMMITTEE:

Supervisor:

(J. Eric Bickel)

(David Morton)

Decision Analysis and Risk Management:
Application to Climate Change and Risk Detection

by

Shubham Agrawal, MS

Thesis

Presented to the Faculty of the Graduate School of

The University of Texas at Austin

in Partial Fulfillment

of the Requirements

for the Degree of

Master of Arts

The University of Texas at Austin

August, 20011

Dedication

I dedicate this thesis to my parents (Mrs. Suman Agrawal and Mr. Manmohan Agrawal) for their love, support and belief in me.

Acknowledgements

I am extremely thankful to Prof. J. Eric Bickel for his support, guidance and advice. I would also like to thank EER program for its support.

Abstract

Decision Analysis and Risk Management: Application to Climate Change and Risk Detection

Shubham Agrawal, MA

The University of Texas at Austin, 2011

Supervisor: J. Eric Bickel

We have analyzed the application of decision analysis and risk management tools to solve practical problems associated with Climate Change and Risk Detection in the financial services industry. Geoengineering, which is described as an intentional modification of earth's environment to mitigate the harmful effects of climate change, is evaluated as a policy alternative using the aforementioned tools. We compared the performance of geoengineering with optimal emission controls and a business as usual strategy under various scenarios and found that geoengineering passes the cost benefit test for a majority of the scenarios. We modified the DICE model (Nordhaus, 2008) and used it to evaluate the performance of different environmental policies. Our results show geoengineering as a potential alternative to solve climate change problems. Through this application, and by comparing our findings against Goes et al. (2011), we showed that how framing of the decision problem can lead to completely different results. We also

analyzed the application of risk management in the financial services industry. The industry faces three main types of risk: Market risk, Credit risk and Operational risk. Market risk is managed using a diversified portfolio, derivatives, insurance and contracts. More challenging is the task of preventing credit and fraud risk. Statistical models used by the industry to detect and prevent these types of risk are explained in the thesis.

Table of Contents

List of Figures

Chapter 1 Introduction

In this thesis, we investigate the applications of tools and techniques used for decision analysis and risk management in making policy decisions for climate change and in detecting credit and fraud risk in the financial services industry. Decision analysis is a set of tools and processes for bringing clarity to complex decisions. The uncertainty involved with most real life decision problems creates risk that can be managed. Risk management involves managing future uncertainties associated with a decision. Thus, decision analysis and risk management are highly correlated; a good decision automatically performs risk management and vice versa. The complexity of real life problems coupled with uncertainty, risk and lack of information increase the importance of a rational decision making framework to help the decision maker choose the best alternative. The process of decision making under risk is as follows:

a) The problem is defined and decision maker uses the information to assign beliefs or subjective probabilities regarding State of the World (SOW), which are different possible scenarios.
b) The payoffs and expected payoffs are calculated for each decision alternative under every SOW.
c) The decision maker chooses the decision that optimizes the expected payoff.

Decision trees, scenario analysis, statistical modeling and simulation are the most popular tools used for decision making and risk management. This thesis details their implementation on practical problems associated with policy decisions for climate change, which is the primary focus of this thesis. However, an application to the financial

sector is also included to show how other more traditional industries benefit from these tools.

This thesis is organized as follows. Chapter 2 describes the climate change problem and the need for an efficient decision framework for policy decisions. It also introduces geoengineering as a viable decision alternative to mitigate climate risk. Chapter 3 details the DICE model which is a mathematical model proposed by Nordhaus (2008) to monetize the impacts of climate change. The modifications made in the DICE model are described in Chapter 4 along with details of its implementation within the DICE model. Experimental design and obtained results are described in Chapter 5. Chapter 6 describes the application of statistical tools to the financial sector to manage risk. Finally Chapter 7 concludes this thesis.

Chapter 2 Climate Change

With increasing anthropogenic emissions of greenhouse gases (GHGs), there is an increasing risk of global warming and its harmful effects. The possibility of abrupt changes in the climate system is driving the scientific community to consider alternative ways of reducing risks posed by anthropogenic carbon emissions (Shepherd et al., 2009). Geoengineering which is described as 'intentional manipulation of the environment to counteract climate change due to anthropogenic emissions' has evolved as a promising approach to minimize damages caused by climate change (IPCC, 2007). Bickel and Lane (2010) performed a cost-benefit analysis of using Solar Radiation Management (SRM) and showed that a continuous use of one watt of SRM results in net savings over $6 trillion under optimal emission controls. They advocated further research in two geoengineering techniques: solar radiation management and air capture to better understand their benefits and side effects.

In this thesis, an economic analysis is performed to estimate the impacts of intermittent aerosol geoengineering (GEO). Goes et al. (2011) (hereby referred to as GTK) have shown that an abrupt turn-off of aerosol geoengineering (due to scenarios like famine, war etc.) can lead to a rapid rise in temperature and can cause more damage than an abatement oriented policy. In this thesis, we show that GTK's conclusions are a result of their framing of the geoengineering use decision.

The way GTK framed the decision problem excludes several possible motivations for geoengineering research and potential deployment:

(i) a concern that emissions reductions may not materialize or that they may not materialize in time (Crutzen, 2006),

(ii) uncertainty regarding the climate sensitivity and the possibility that the climate may be more sensitive to greenhouse gasses (GHG) than some fear, and

(iii) a belief that the climate system may contain tipping points beyond which significant and irreversible damages may occur (Lenton et al., 2008).

In addition, GTK have completely substituted abatement with geoengineering and used very high levels of abatement (enough to keep the forcing at preindustrial levels) in their research. They compared this policy of no controls to a policy of "optimal" and strong emissions controls (e.g., GTK's abatement strategy called for a 25% reduction in global CO_2 emissions by 2015 and 40% by 2025). Since a policy of no controls is, by definition, economically worse than optimal controls, especially given GTK's assumptions, burdening a decision to use GEO with the decision to pursue no controls biases the results against the use of GEO. GTK's framing also assumes continuous emission abatement, an inability to respond to shut-down of GEO and no negative externalities as a result of emission control.

In our opinion, geoengineering should not be used to substitute abatement, but it should be used with abatement to reduce the damages. Drastic situations which can demand turning off of geoengineering can also demand turning off of abatement. For example, an economic crisis can force the government to reduce/remove any carbon tax and jeopardize abatement. Therefore, a comparison of intermittent geoengineering with constant abatement is not justifiable.

GTK also claim that the DICE model, in its current form, has a few shortcomings namely, a rate independent damage function, fixed monetary discount rates over time and coarse climate model, limiting its ability for this analysis and they proposed some

modifications. GTK argued that damage function used in the DICE model (Nordhaus, 2008) depends only on the deviation of the global mean surface temperature from the preindustrial value and neglects the importance of the rate of climate change. Rate of climate change, according to several experts, is an important factor in determining climatic damage as a large portion of the climate damage comes from the inability to adapt to the change. If the rate of change is slow, the damage is expected to be low since society can adapt to it with time. A high rate of change will make the adaptation hard and therefore result in greater damage. Since, an abrupt turn-off of geoengineering is likely to produce warming at a higher rate, GTK advocated the use of a rate dependent climate damage function in DICE and substituted the DICE damage function with a rate dependent damage function proposed by Lempert et al. (2000).

GTK also suggested that the discounting used in DICE is not suitable for long time horizons. The fixed monetary discount rates were substituted with rates based on a random walk model reported by Newell and Pizer (2004), hereby referred as N&P. In addition, GTK claimed that the climate model used in DICE represents poorly the effects of fast changes in radiative forcing that would occur during abrupt termination of geoengineering and replaced it with the DOECLIM (Diffusion Ocean Energy Balance Climate Model) by Kriegler (2005). They claim that aerosol geoengineering is cost effective only if it is applied continuously with zero probability of turn-off.

In this thesis, we do not argue for or against GEO deployment/research but aim to provide a rational decision framework to evaluate the costs and benefits of geoengineering. We show how a different, and possibly more reasonable, framing, using GTK's own assumptions and model formulation, demonstrates that GEO passes a cost-benefit test over the wide range of scenarios that they considered.

In addition, we have also analyzed the individual impacts of each change made to the DICE model in order to ascertain their contribution to the difference in results. The results obtained using DICE with and without Lempert's damage functions (2000) are not substantially different indicating that rate of temperature change does not have a big impact on the working of model. Similar results are obtained when the DICE climate function is substituted with DOECLIM. However, the change in discount rate from DICE to N&P results in a completely different set of results. The results indicate that of all the modifications made in DICE by GTK, the discount rate is the most important. The influence of the damage function and DOECLIM on the results is seen when they are used together since the damage function needs a fine temperature model to capture the rate of change.

Chapter 3 Dynamic Integrated Model of Climate and Economy

The Dynamic Integrated Model of Climate and the Economy (DICE) is an economic optimal-growth model that combines a global carbon cycle, the climate system, and the economic impacts of climate change. It relates economic growth to CO_2 emissions, CO_2 emissions to temperature change, and temperature change to climate damage. The model is briefly described below (a more detailed description of the model can be found in Nordhaus, 2008).

3.1 THE ECONOMIC MODEL

The DICE model is aimed at maximizing the generalized level of consumption now and in the future. For this purpose, mathematically, the objective of the DICE model is to maximize a social welfare function that is the discounted sum of utility of consumption. This social welfare function is represented as a relationship between three basic value judgments:

- Higher levels of consumption have higher worth.
- Marginal value of consumption decreases with increase in consumption.
- Society will undertake investments to increase consumption in periods where marginal utility of consumption is highest.

Thus, the objective function is the discounted sum of utility of consumption *U[c(t), L(t)]* given as:

$$\max_{\{c(t)\}} \sum_t U[c(t), L(t)]R(t), \tag{3.1}$$

where, *U* is utility, *c(t)* is the per capita consumption at time *t*, *L(t)* represents the population (labor input) at time *t*, and *R(t)* is the discount factor which is a function of pure rate of social time preference (ρ):

$$R(t) = (1+\rho)^{-t}. \quad (3.2)$$

The model operates in time steps of 10 years. Another convention the model follows is that stocks are measured at the beginning of each period. The utility function is defined as an isoelastic function of marginal utility of consumption, α:

$$U[c(t), L(t)] = L(t)\{[c(t)]^{1-\alpha} - 1\}/(1-\alpha). \quad (3.3)$$

Total output *Q(t)* is assumed to be a constant-returns to scale Cobb-Douglas production functions of capital *K(t)*, labor *L(t)*, and Hicks neutral technological change *A(t)* and is given as:

$$Q(t) = \Omega(t)[1-\Lambda(t)]A(t)K(t)L(t)^{1-\gamma}, \quad (3.4)$$

where, γ is the elasticity of output with respect to capital. The economic impacts of climate change and investments in CO_2 abatement are represented by damage function *Ω(t)* and abatement cost function *Λ(t)*, respectively. The damage function assumes that climate damages are proportional to world output and result from surface temperature changes and therefore can be represented as a polynomial function of global mean surface temperature change $T_{AT}(t)$ (^{o}C rise from year 1750):

$$\Omega(t) = 1/[1 + \psi_1 T_{AT}(t) + \psi_2 T_{AT}(t)^2], \quad (3.5)$$

where, ψ_1 and ψ_2 are estimated through empirical studies to be 0 and 0.0028, respectively. The abatement cost function assumes that abatement costs are proportional to global output and calculates the cost of emissions reduction as a polynomial function of emissions reduction rate *μ(t)*:

$$\Lambda(t) = \pi(t)\theta_1(t)\mu(t)^{\theta_2}. \quad (3.6)$$

$\pi(t)$ is participation cost markup, which is an abatement cost with incomplete participation as a fraction of abatement cost with complete participation while $\theta_1(t)$ and θ_2 are parameters of the abatement cost function.

Consumption *C(t)* is defined as the part of output that is not devoted to investment *I(t):*

$$C(t) = Q(t) - I(t). \quad (3.7)$$

Thus, per capita consumption *c(t)* can be given as:

$$c(t) = C(t)/L(t). \quad (3.8)$$

Investment at any period contributes to capital stock at the beginning of the next period and depreciates at a constant rate (δ_k):

$$K(t) = I(t-1) + (1- \delta_k)K(t-1). \quad (3.9)$$

Uncontrolled industrial emissions are obtained by multiplying the exogenously determined carbon intensity of economic activity $\sigma(t)$ by the total world output:

$$E_{Ind}(t) = \sigma(t)[1 - \mu(t)]A(t)K(t)^{\gamma}L(t)^{(1-\gamma)}. \quad (3.10)$$

The DICE model assumes that total resources of carbon fuel are limited by *CCum* and puts a constraint on the total emissions:

$$CCum \geq \sum_{t=0}^{Tmax} E_{Ind}(t). \quad (3.11)$$

The total CO_2 emissions is given as sum of industrial and land-use (deforestation, landslides etc.) emissions:

$$E(t) = E_{Ind}(t) + E_{Land}(t). \quad (3.12)$$

T_{max} is the time period for which the model will be executed (600 years).

3.2 THE CARBON CYCLE MODEL

Emissions of CO_2 by humans increases the atmospheric CO_2 stock (M_{AT}). DICE models the global carbon cycle by a three reservoir system. The three reservoirs for carbon are: the atmosphere, a quickly mixing reservoir in upper oceans and biosphere, and the deep ocean. DICE uses a first-order, linear, three-box model (reservoir representing boxes) to model the effects of anthropogenic emissions on global mean carbon cycle. CO_2 stock in a reservoir at the beginning of time period *t* is given as the sum of CO_2 stock at period *t*-1, the amount of CO_2 added directly to the reservoir during period *t*-1 and additional CO_2 added as a result of mixing between the two reservoirs. It is mathematically represented as:

$$M_{AT}(t) = E(t-1) + \emptyset_{11} M_{AT}(t-1) + \emptyset_{21} M_{UP}(t-1), \quad (3.13)$$

$$M_{UP}(t) = \emptyset_{22} M_{UP}(t-1) + \emptyset_{32} M_{Lo}(t-1) + \emptyset_{12} M_{AT}(t-1), \quad (3.14)$$

$$M_{Lo}(t) = \emptyset_{33} M_{Lo}(t-1) + \emptyset_{23} M_{UP}(t-1), \quad (3.15)$$

where, $M_{AT}(t)$, $M_{UP}(t)$, and $M_{Lo}(t)$ represent the mass of carbon in reservoir for atmospheric, upper oceans, and lower oceans respectively. $\emptyset_{ij}$ are parameters of the carbon cycle and refer to transfer rates of CO_2 between reservoirs.

3.3 THE CLIMATE MODEL

The net radiative forcing *F(t)* due to CO_2 concentration above pre-industrial level ($M_{AT}(1750)$) is given as:

$$F(t) = F_{2xCO_2} \left\{ log_2 \left[\frac{M_{AT}(t)}{M_{AT}(1750)} \right] \right\} + F_{EX}(t). \quad (3.16)$$

F_{2xCO_2} is the radiative forcing for a doubling of CO_2 concentrations and is assumed to be 3.8 W/m^2. $F_{EX}(t)$ represents the forcing of non-CO_2 GHGs and the negative forcing due to aerosols.

DICE uses a simple two-box climate model that provides a reasonable approximation of climate change response to anthropogenic forcing:

$$T_{AT}(t) = T_{AT}(t-1) + \xi_1\{F(t) - \xi_2 T_{AT}(t-1) - \xi_3[T_{AT}(t-1) - T_{Lo}(t-1)]\}, \quad (3.17)$$

$$T_{Lo}(t) = T_{Lo}(t-1) + \xi_4[T_{AT}(t-1) - T_{Lo}(t-1)]. \quad (3.18)$$

$T_{AT}(t)$ and $T_{Lo}(t)$ denote the increase in global mean surface temperature and temperature of lower oceans from 1990. ξ_i are parameters of the climate equation.

Chapter 4: Modifications made to DICE

This chapter describes the modifications made to DICE to study intermittent geoengineering. Several key components of the DICE model have been modified as suggested by GTK to make it more accurate for this analysis.

4.1 Rate Dependent Damage Function

Application of SRM leads to a decrease in the amount of radiation reaching the earth's surface which helps to mitigate the greenhouse heating done by anthropogenic carbon-dioxide. The climate damage as calculated in DICE is a quadratic function of the increase in temperature relative to that of the preindustrial age. SRM lowers radiative forcing which lowers temperature. However, if SRM is stopped it can lead to a rapid rise in temperature. One of the drawbacks of the DICE damage function as pointed by GTK is its inability to account for damage due to the rate of change of temperature. Expert surveys in the past (Nordhaus, 1994) have indicated that climate damage not only depends on the change in temperature but also upon the rate of change of temperature. Therefore, in this thesis a rate dependent damage function proposed in Lempert et al. (1998) has been used. The new damage function is given as:

$$\Omega(t) = \frac{1}{\tanh\left(\alpha_1\left[\frac{\Delta\overline{T}_5(t)}{3℃}\right]^{\eta_1} + \alpha_2\left[\frac{\Delta T(t) - \Delta\overline{T}_{30}(t)}{0.35℃}\right]^{\eta_2}\right)}. \quad (4.1)$$

$\Omega(t)$ measures the climate damages as a fraction of gross world output, $\Delta T(t)$ is the global mean surface temperature change, $\Delta\overline{T}_5(t)$ and $\Delta\overline{T}_{30}(t)$ are five and 30-year running averages of $\Delta T(t)$ respectively, α_1 and α_2 are scaling factors and η_1 and η_2 are exponents that determine the non-linearity of the relationship. The first term in the denominator of equation (4.1) represents the economic damages due to the change in global mean surface temperature and is similar to power law functions used in the literature for damage models. The second term in the denominator represents the climate

damage due to long term climate variations. The hyperbolic tangent is added to maintain numeric stability. Equation (4.1) replaces equation (3.5) of the DICE model. For the sake of implementation in the DICE model (since the model runs in time periods of 10 years), $\Delta T(t)$ and $\Delta \overline{T}_5(t)$ are taken equal to $T_{AT}(t)$, which is global mean surface temperature change per decade (difference between global mean surface temperature in decade '*t*' and the preindustrial value). Thereby, $\Delta \overline{T}_{30}(t)$ is calculated as the running average of global mean surface temperature of three consecutive decades.

The selection of the α_1, α_2, η_1, η_2 parameters is very important for the new damage function. GTK derived the values of α_1, α_2 by fitting the damage function to the expert assessments by Nordhaus (1994)[1]. We executed the DICE model (with no SRM) with Lempert's damage function and the values obtained from each expert assessment. The obtained results are shown in Figure 4.1. The figure gives an idea of the amount of variation that exists between different expert opinions. While some expert argues in favor of high damage (to the order of $83 trillion dollars) due to climate change, there are experts who estimated total climatic damage to be quite low ($0.1 trillion). These differences exist due to the difference in opinion regarding the influence of climate on day to day life and the human adaptability to climate change. None of the expert assessments can be thought of as better compared to the others due to the subjectivity of the matter, making the task of choosing a suitable scaling factor complex.

To address this issue, in this thesis, all 18 estimates are assumed to be equally likely. The values of η_1 and η_2 are taken as 2 and 4, respectively, consistent with the literature.

[1] Nordhaus (1994) surveyed a panel of 19 experts – 10 economists, four social scientists and five natural scientists about the economic impacts, distributional effects and non-market effects of global warming. They considered three scenarios: 3°C warming by 2090 (A), 6°C warming by 2175 (B), and 6°C warming by 2090 (C).

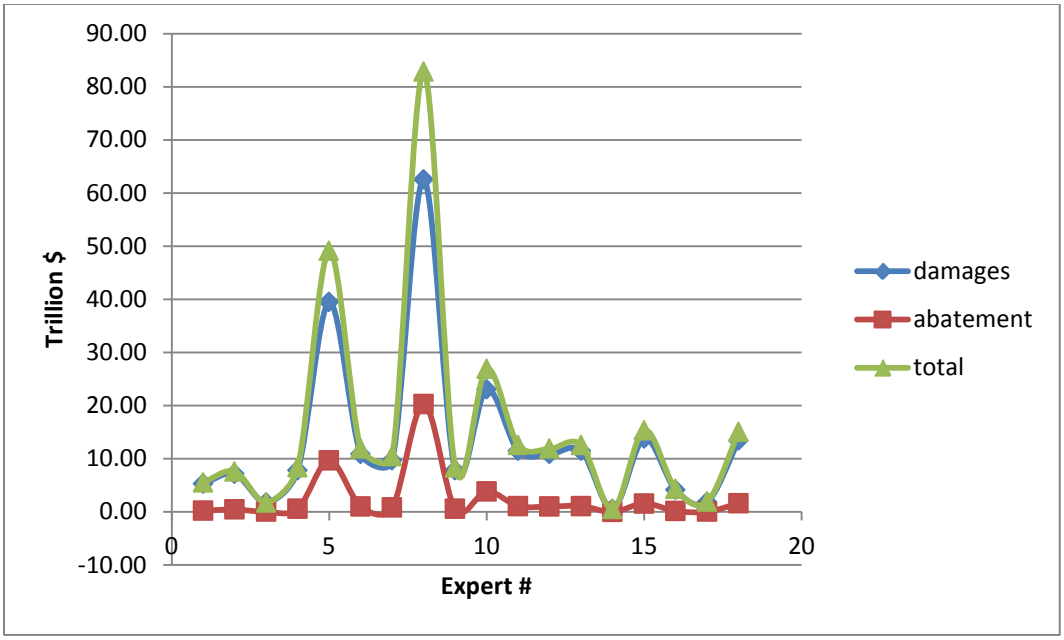

Figure 4.1 NPVs of damage obtained by using different scaling factors derived using experts' opinion in the DICE model.

4. 2. MODIFICATIONS IN MONETARY DISCOUNT RATES

DICE uses a fixed value of social rate of time preference ρ to calculate the social time preference discount factor $R(t) = (1+\rho)^{-t}$. Generally, when valuing a future, one uses the average discount rate (i.e., if discount rates are assumed to vary from 1-7% then 4% is assumed to be the average discount rate for the calculations). N&P claimed that this is not the case when long horizons are considered. They showed that for the long term future, the effective discount rate is the lower value of discount rate, not the average value because the higher rate discounts the benefits to such an extent that they add very little to the expected value. However, Gollier and Weitzman (2010) have recently shown that the N&P framework assumes there is an immediate and permanent dislocation in the return to capital. Gollier (2009) proved that if uncertainty in returns is transitory, for

example, if it follows Geometric Brownian Motion, as assumed by N&P, then the term-structure of interest rates should be flat, as originally assumed by Nordhaus (2008).

GTK used the N&P value of the discount factor as a benchmark to calculate an exponentially decaying social rate of time preference ρ(t) for each period. Therefore, in this thesis, to benchmark GTK, we use an exponentially decreasing social rate of time preference. But we will also check the sensitivity of our results with respect to this assumption on discounting. In our model we also changed the constant social time preference factor 'ρ' in equation (3.2) with a time dependent exponentially decaying parameter 'ρ(t)'.To calculate the social time preference decline rate, we have fit the discount factor obtained from N&P in a least square sense with the obtained fit is shown in Figure 4.2. The values of initial social time preference and social time preference decline rate is also changed in DICE model as per the results obtained from the least square fit using a constant elasticity of marginal utility of consumption (α) value of 1.1.

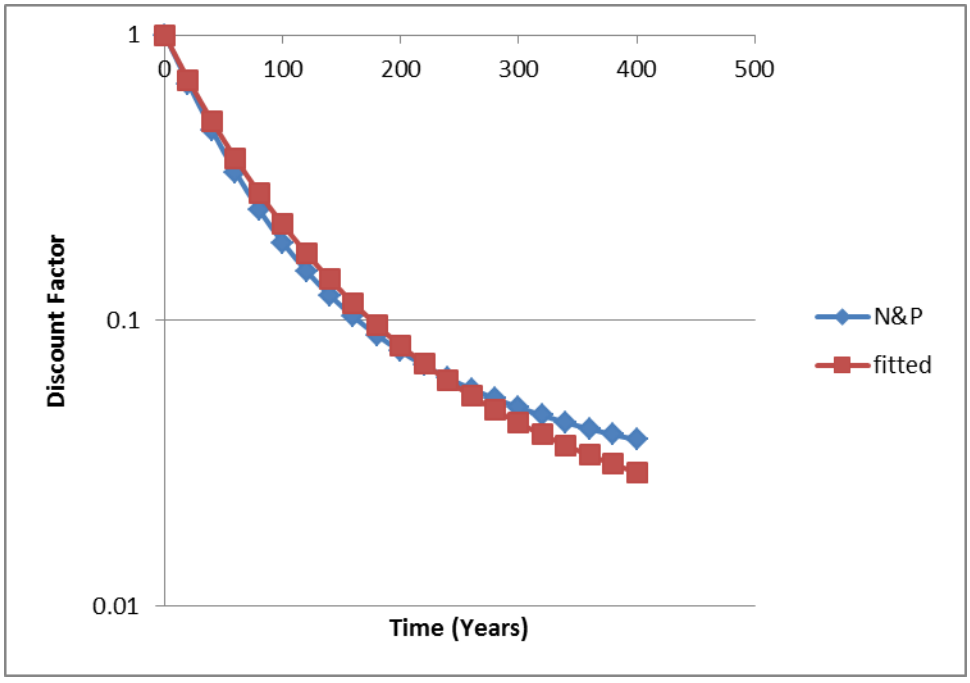

Figure 4.2 Monetary discount factors from the Newell and Pizer (2004) and obtained fit.

4.3 MODIFICATION IN CLIMATE MODEL

GTK claimed that the climate model in DICE is coarse and as such is not suitable for calculating temperature change due to abrupt turning off of SRM. They replaced the two-box climate model in DICE with DOECLIM (Diffusion Ocean Energy Balance Climate Model) proposed by Kriegler (2005) which is a four-box model and can capture the sharp hike in temperature effectively.

4.3.1 DOELCIM

DOECLIM is an energy-balance model that calculates the response of surface temperature to changes in radiative forcing. In equilibrium, the amount of infrared radiation F_S emitted at the earth surface equals the sum of solar radiations F_{sol} absorbed by it and extra energy G that is absorbed by the atmosphere and later distributed to the earth surface, i.e.,

$$F_S = F_{sol} + G, \tag{4.2}$$

or, $$\sigma T_{S,eq}{}^4 = F_{sol} + G. \tag{4.3}$$

Equation (4.3) is the Stefan-Boltzmann Law, which assumes the earth's surface radiates like a blackbody. The heating done by G is known as greenhouse effect. A perturbation in incident energy disturbs the equilibrium and generates a heat flux $\dot{H}$, the first order Taylor approximation of which is given as:

$$\dot{H}(t) = \Delta E(t) - 4\sigma\left(T_{S,eq}\right)^3 \Delta T_S(t). \tag{4.4}$$

ΔE(t) is the change in incident energy and ΔT_S is surface temperature change with respect to the equilibrium temperature (preindustrial age for climate change purposes). Energy Balance Models (EBMs) of climate change assume that this change in incident energy can be approximated by the change in radiative forcing and a temperature feedback term which scales with the temperature anomaly.

$$\dot{H}(t) = Q(t) - \lambda \Delta T_S(t). \tag{4.5}$$

The change in radiative forcing $Q(t)$ can be measured as the sum of changes in incident solar radiation, changes in aerosol and GHG concentrations. Thus,

$$\dot{H}(t) = Q_{Atm}(t) + Q_{Alb}(t) + Q_{Sol}(t) - \lambda \Delta T_S(t), \quad (4.6)$$

where, $Q_{Atm}(t), Q_{Alb}(t), Q_{Sol}(t)$ are radiative forcing due to changes in atmospheric parameters, changes in albedo parameters and changes in incident solar activity, respectively. λ is the climate feedback strength parameter.

Since the heat flux is dominated by oceans, a realistic energy balance model needs to consider ocean and land separately. Therefore, DOECLIM separates ocean and land and in its initial form is comprised of four-boxes: land (L), troposphere over land (AL), troposphere over sea (AS), and ocean mixed layer (S). The radiative heating is distributed between these four boxes before diffusing into interior oceans:

$$Troposphere\ (Land):\ C_A \dot{T}_{AL} = Q^*_{AL} - \lambda^*_{AL} T_{AL} - \frac{k^*}{f_L}(T_{AL} - T_{AS}) - k^*_L (T_{AL} - T_L), \quad (4.7)$$

$$Land: C_L \dot{T}_L = Q^*_L - \lambda^*_L T_L - k^*_L (T_L - T_{AL}), \quad (4.8)$$

$$Troposphere\ (Sea):\ C_A \dot{T}_{AS} = Q^*_{AS} - \lambda^*_{AS} T_{AS} - \frac{k^*}{1 - f_L}(T_{AS} - T_{AL}) - k^*_S (T_{AS} - T_S), \quad (4.9)$$

$$Ocean\ mixed\ layer:\ c_V z_S \dot{T}_S = Q^*_S - \lambda^*_S T_S - k^*_S (T_S - T_{AS}) - F_{O,} \quad (4.10)$$

where, $\lambda^*_{AL}, \lambda^*_{L,}\ \lambda^*_{AS}$, and λ^*_S are climate feedback parameters for troposphere over land, land, troposphere over sea and sea, respectively in $Wm^{-2}K^{-1}$; k^* is an atmospheric land sea heat exchange coefficient in $Wm^{-2}K^{-1}$; k^*_L and k^*_S are atmosphere-land and atmosphere-sea heat exchange coefficients in $Wm^{-2}K^{-1}$; F_O is heat flux in interior oceans in Wm^{-2}; c_V is the specific heat capacity of sea water; z_S is the depth of the ocean mixed layer in m; C_A and C_L are the heat capacity of the atmosphere and land in $W.yr/(m^2K^1)$; $Q^*_{AL}, Q^*_L, Q^*_{AS}, Q^*_S$ are radiative forcing in Wm^{-2}; and f_L is the land fraction of the earth's surface.

Equations (4.7)–(4.10) have the basic structure of equation (4.5) separated into different boxes and also include heat transfer into neighboring boxes. It is assumed that no direct heat transfer takes place between land and ocean. Taking advantage of

proportionality between surface and troposphere warming (due to strong coupling between surface and troposphere), the four box model can be reduced into a two-box model as:

$$Land + Troposphere \quad C_{AL}\dot{T}_L = Q_L - \lambda_L T_L - \frac{k(T_L - b_{SI}T_S)}{f_L}, \tag{4.11}$$

$$Ocean + Troposphere \quad C_{AS}\dot{T}_S = Q_S - \lambda_S T_S - \frac{k(b_{SI}T_S - T_L)}{1 - f_L} - F_O. \tag{4.12}$$

$C_{AL} = aC_A + C_L$ represents effective heat capacities of troposphere and land, while $C_{AS} = ab_{SI}C_A + c_V z_S$ represents the effective heat capacity of ocean and land. Climate feedback parameters for surface-troposphere system over land are given by $\lambda_L = a\lambda_{AL}^* + \lambda_L^*$ and over ocean by $\lambda_S = ab_{SI}\lambda_{AS}^* + \lambda_S^*$; $k = ak^*$ is the land sea heat exchange coefficient relative to the surface air temperature gradient; $Q_L = Q_{AL}^* + Q_L^*$ and $Q_S = Q_{AS}^* + Q_S^*$ are the radiative forcing at land and sea surface respectively. $a = 1.2$ is the troposphere warming enhancement while b_{SI} represents air warming enhancement from retreating sea ice (i.e., the ratio between global mean marine surface air temperature anomaly and global mean SST).

Heat uptake by the ocean plays an important role in the functioning of any EBM and therefore efficient modeling of heat flux F_O is crucial. Kriegler (2005) employed a 1-D upwelling diffusion model to model the penetration of heat anomaly into the ocean due to rising surface temperature and derived an analytical solution of the problem (Kriegler, 2005 appendix B) given as:

$$F_O(t) = f_{SO}c_V\sqrt{\frac{\kappa_V}{\pi}}\int_o^t \frac{\dot{T}_S(t')}{\sqrt{t - t'}}\left(1 + 2\sum_{n=1}^{+\infty}(-1)^n exp\left(-\frac{n^2 z_B^2}{\kappa_V(t - t')}\right)\right)dt'. \tag{4.13}$$

κ_V is the effective vertical diffusivity of heat in cm^2sec^{-1}, f_{SO} is a scaling factor that captures the reduction area at the bottom of the mixed layer relative to ocean surface area (to account for shallow coastal water where heat cannot pass into interior oceans), and z_B is the point at which heat flux into ocean floor vanishes.

4.3.2 Model Calibration

Equations (4.11)-(4.13) comprise the core of the DOECLIM. The goal of model calibration is to reduce the number of free model parameters to two: global climate sensitivity (T_{2x}) and ocean vertical diffusivity (κ_V). An overview of the main results from the literature is provided here; the detailed calibration procedure is explained in Kriegler (2005) Appendix A. The parameters f_L and f_{SO} are derived directly from the topography of earth, z_B = 4000m is close to average ocean depth and has been used frequently in the literature. Seasonal data has been used to obtain the value of *k*, C_{AL} and C_{AS}. The expression for *k* thus obtained is

$$k = b_k - a_k \lambda_L, \tag{4.14}$$

where, b_k = 1.59 $Wm^{-2}K$ and a_k = 0.31. The remaining three parameters λ_L, λ_S and b_{SI} cannot be estimated from seasonal data because they refer to climate system properties from decadal to secular time scale. Data from the CLIMBER-2 (Schneider von Deimling et al., 2006) experiment is used to fix the value of b_{SI} at 1.3. The value of *k*, $\lambda_L, and\ \lambda_S$ can be derived using an equilibrium solution to equations (4.11), (4.12) and (4.14) as:

$$\lambda_L = f_L \frac{R_\lambda f_L + (1 - f_L) b_{SI}}{R_\lambda f_L - a_k (R_\lambda - b_{SI})} \frac{Q_{2x}}{T_{2x}} - b_k \frac{R_\lambda - b_{SI}}{R_\lambda f_L - a_k (R_\lambda - b_{SI})}, \tag{4.15}$$

$$\lambda_S = \left(R_\lambda f_L - a_k \frac{R_\lambda - b_{SI}}{1 - f_L} \right) \frac{R_\lambda f_L + (1 - f_L) b_{SI}}{R_\lambda f_L - a_k (R_\lambda - b_{SI})} \frac{Q_{2x}}{T_{2x}} + \frac{R_\lambda f_L}{1 - f_L} b_k \frac{R_\lambda - b_{SI}}{R_\lambda f_L - a_k (R_\lambda - b_{SI})}, \tag{4.16}$$

$$k = b_k \frac{R_\lambda f_L}{R_\lambda f_L - a_k (R_\lambda - b_{SI})} - a_k f_L \frac{R_\lambda f_L + (1 - f_L) b_{SI}}{R_\lambda f_L - a_k (R_\lambda - b_{SI})} \frac{Q_{2x}}{T_{2x}}, \tag{4.17}$$

where, R_λ = 1.43 is the land enhancement factor.

4.3.3 Numerical Implementation of DOECLIM

In order to numerically integrate equations (4.11) and (4.12), a range of time scales present in the model needs to be assessed. DOECLIM contains six time scales,

$$\tau_L = \frac{C_{AL}}{\lambda_L},\ \tau_{LS} = f_L\frac{C_{AL}}{k},\ \tau_{BO} = \frac{z_B^2}{\kappa_V},\ \tau_S = \frac{C_{AS}}{\lambda_S}, \tau_{SL} = (1-f_L)\frac{C_{AS}}{\lambda_S}, \tau_{FO} = \left(\frac{C_{AS}}{c_V}\right)^2\frac{\pi}{\kappa_V}. \quad (4.18)$$

These time scales vary from 1-2 months to 10-30 years. Equations (4.11) and (4.12) can be written in terms of these time scales as:

$$\dot{T}_L = \frac{Q_L}{C_{AL}} - \frac{T_L}{\tau_L} - \frac{T_L - b_{SI}T_S}{\tau_{LS}}, \quad (4.19)$$

$$\dot{T}_S = \frac{Q_S}{C_{AS}} - \frac{T_S}{\tau_S} - \frac{b_{SI}T_S - T_L}{\tau_{SL}} - \frac{f_{SO}}{\sqrt{\tau_{FO}}}\int_0^t \frac{\dot{T}_S(t')}{\sqrt{t-t'}}\left(1 + 2\sum_{n=1}^{\infty}(-1)^n exp\left(-\frac{n^2\tau_{BO}}{t-t'}\right)\right)dt'. \quad (4.20)$$

Due to variation of time scale over two orders of magnitude, equations (4.19) and (4.20) constitute a system of stiff differential equations. Kriegler (2005) used an implicit numerical integration technique, one-stage Runge Kutta method, to integrate the system in time intervals of 1 year resulting in following discrete time numerical representation of time continuous model described by equations (4.19) and (4.20),

$$B\begin{pmatrix} T_{L,i+1} \\ T_{S,i+1} \end{pmatrix} = Q + A\begin{pmatrix} T_{L,i} \\ T_{S,i} \end{pmatrix}, \quad (4.21)$$

where, *B* and *A* are following 2x2 matrices, and Q the following two-dimensional vector:

$$B = \begin{pmatrix} 1 + \frac{1}{2}\frac{\Delta t}{\tau_L} + \frac{1}{2}\frac{\Delta t}{\tau_{LS}} & -\frac{1}{2}\frac{\Delta t}{\tau_{LS}}b_{SI} \\ -\frac{1}{2}\frac{\Delta t}{\tau_{SL}} & 1 + \frac{1}{2}\frac{\Delta t}{\tau_S} + \frac{1}{2}\frac{\Delta t}{\tau_{SL}}b_{SI} + f_{SO}\sqrt{\frac{\Delta t}{\tau_{FO}}}a_0 \end{pmatrix},$$

$$Q = \begin{pmatrix} \frac{\Delta t}{2}\frac{Q_L\left(t_i + \frac{\Delta t}{2}\right)}{C_{AL}} \\ \frac{\Delta t}{2}\frac{Q_S\left(t_i + \frac{\Delta t}{2}\right)}{C_{AS}} + f_{SO}\sqrt{\frac{\Delta t}{\tau_{FO}}}\sum_{j=1}^{i-1}\left(a_{i-j} - a_{i-j+1}\right)T_{S,j} \end{pmatrix},$$

$$A = \begin{pmatrix} 1 - \frac{1}{2}\frac{\Delta t}{\tau_L} - \frac{1}{2}\frac{\Delta t}{\tau_{LS}} & \frac{1}{2}\frac{\Delta t}{\tau_{LS}}b_{SI} \\ \frac{1}{2}\frac{\Delta t}{\tau_{SL}} & 1 - \frac{1}{2}\frac{\Delta t}{\tau_S} - \frac{1}{2}\frac{\Delta t}{\tau_{SL}}b_{SI} + f_{SO}\sqrt{\frac{\Delta t}{\tau_{FO}}}(a_0 - a_1) \end{pmatrix},$$

and, $a_{i-j} = \int_j^{j+1} \frac{1+2\sum_{n=1}^{\infty}(-1)^n exp\left(-\frac{n^2\tau_{BO}}{\Delta t}\frac{1}{i+1-l'}\right)}{\sqrt{i+1-l'}} dl'$

$= 2\sqrt{i-j+1}\left(1+2\sum_{n=1}^{\infty}(-1)^n\, exp\left(-\frac{n^2\tau_{BO}}{\Delta t}\frac{1}{i-j+1}\right)\right) - 2\sqrt{i-j}\left(1+\right.$

$\left.2\sum_{n=1}^{\infty}(-1)^n\, exp\left(-\frac{n^2\tau_{BO}}{\Delta t}\frac{1}{i-j}\right)\right) + 4\sum_{n=1}^{\infty}(-1)^{n+1} n\sqrt{\pi\frac{\tau_{BO}}{\Delta t}}\left(Erf\left(n\sqrt{\frac{\tau_{BO}}{\Delta t}\frac{1}{i-j}}\right) -\right.$

$\left.Erf\left(n\sqrt{\frac{\tau_{BO}}{\Delta t}\frac{1}{i-j+1}}\right)\right).$

Erf in the aforementioned equations represents the error function. Given $T_{L,\,i}$ and $T_{S,\,i}$ values for $i = 0$, the temperature for any given i can be calculated recursively by solving,

$$\begin{pmatrix} T_{L,i+1} \\ T_{S,i+1} \end{pmatrix} = B^{-1}\left(Q + A.\begin{pmatrix} T_{L,i} \\ T_{S,i} \end{pmatrix}\right). \quad (4.22)$$

The global mean surface temperature is then calculated using,

$$T_i = f_L T_{L,i} + (1-f_L) T_{S,i}\,. \quad (4.23)$$

4.3.4 Integration with DICE

The integration of DOECLIM with DICE poses a challenge due to different time scales of both the models. While DICE run in steps of 10 years, DOECLIM is designed to run in time steps of 1 year. Our DOECLIM implementation in DICE is carried out by making a few assumptions. Like most other climate models, DOECLIM only requires the value of net radiative forcing of the $(i+1)^{st}$ year and temperature of the i^{th} year to output temperature of the $(i+1)^{st}$ year. The DICE model calculates the value of radiative forcing for each decade, which acts as input to DOECLIM. We assume that radiative forcing will stay constant during the decade, i.e., the same for each year of that decade. Using this assumption, the values of radiative forcing from DICE and initial change in temperature, the DOECLIM model predicts the temperature change in following years. The temperature change values from DOECLIM acts as input to DICE which in turn calculates the emission control rates and predict the radiative forcing for the next decade.

We have implemented DOECLIM in the DICE model using both GAMS and MS Excel. GAMS implementation of the model uses the CONOPT solver for optimization and calculates optimal emission control rates along with other parameter values while we use Excel with a predefined emission control trajectory to calculate and output the parameter values.

4.4 INCORPORATION OF SRM

In order to incorporate SRM in DICE, the forcing equation (3.16) is modified as in Bickel and Lane (2010):

$$F(t) = F_{2xCO_2}\left\{\log_2\left[\frac{M_{AT}(t)}{M_{AT}(1750)}\right]\right\} + F_{EX}(t) - SRM(t), \qquad (4.24)$$

where, $SRM(t)$ represents the amount of negative forcing due to solar radiation management.

Chapter 5 Results and Discussion

In this chapter, we analyze the benefits and limitations of SRM using the modified DICE model and a wide range of decision scenarios. In addition, we test the relative importance of modifications made to DICE.

5.1 Drawbacks In GTK's Cost/Benefit Analysis

Goes et al. (2011) conducted an economic analysis and showed that the damage due to a potential turning-off of SRM can outweigh the benefits. GTK concluded that if the chances of aborting SRM are greater than 15%, or if the damages caused due to side effects of SRM implementation are greater than half a percent of the world's economy, then an optimal emission reduction policy would be economically more profitable. However, GTK's economic analysis contains a number of assumptions that bias the results in favor of emission abatement.

5.1.1 SRM in not an 'OR' it's an 'AND'

In their paper, GTK compared SRM with no abatement against an optimal abatement policy. We emphasize the use of geoengineering with abatement to achieve a long term, effective and pragmatic solution to climate change, which cannot be obtained using abatement or SRM alone. Thus, in our decision framework, we consider emission abatement with geoengineering to provide a more rational overview of using geoengineering.

5.1.2 Biased Intermittent SRM policy interpretation

GTK have claimed that unforeseen circumstances (war, breakdown of international agreement, etc.) can demand shutting down SRM forcing and cause abrupt warming and therefore large economic damages. GTK then compared the policy of intermittent geoengineering with continuous abatement. First, we argue that similar situations may also demand aborting an emission reduction policy – a possible scenario

which GTK ignored completely. Second, in their economic analysis GTK compared the utility of using geoengineering with no controls for 50 years against a policy of optimal controls for 600 years. In our view, this amounts to an unfair comparison because of much longer time frame for emission controls which biases the results in favor of an optimal control policy. In our view, a fair comparison requires involved policies to be implemented for same duration. We address this issue in this thesis by modifying an intermittent SRM strategy such that optimal emission controls are enforced once SRM is turned off. We also investigate the decision scenario where optimal controls are aborted after implementation.

5.1.3 Impractical Emission Control Rates

The optimal emission control rates used in GTK are very high compared to those obtained by the DICE model. In our opinion, implementing a policy with such a high emission control rate on a global level is impractical in the near future.

5.1.4 High Level of SRM

The SRM forcing used in GTK counteracts the CO_2 radiative forcing completely. Bickel and Lane (2010) have shown that a low amount of SRM forcing (one, two and three W/m^2) can also be used to reduce the impact of anthropogenic CO_2. If used continuously, higher values of SRM forcing gives better results given there are no side effects of deploying SRM. However, in case there is a possibility of shut down and side effects, lower amounts of SRM can produce better results. Therefore, in this thesis, we also consider decision scenarios with fixed 1 W/m^2 of SRM used along with abatement.

5.2 Experimental Design

The main environmental policy alternatives studied in the thesis are: Business As Usual (BAU), Optimal Controls (OC), Continuous SRM (Cont. GEO), and Intermittent SRM (Interm. GEO). Under the business as usual strategy, no emission control takes place and emission controls rates are assumed zero throughout. Our optimal control

policy uses emission controls to maximize the combined utility of current and future generations. Continuous GEO utilizes SRM forcing to completely offset anthropogenic forcing and assumes that geoengineering will continue forever. Intermittent geoengineering assumes aborting geoengineering after a certain period of time. The time of aborting SRM is taken as 50 years after its implementation beginning in 2015 i.e., in 2065. An increase in deployment time for SRM only tends to bias the results in favor of geoengineering (because SRM offers benefits and is assumed completely free, a longer usage results in higher utility). All the decision scenarios use these policies or their variations.

We compare the performance of each strategy using parameters like total discounted utility of consumption, net NPV of damage and abatement, emission control rates, global mean surface temperature change, rate of temperature change, and net radiative forcing. Following GTK, we consider the uncertainty in three important model parameters: climate sensitivity, climate damages and abatement costs. Uncertainty in climate sensitivity is incorporated by using a probability density function for climate sensitivity and 50 discrete equally likely values are selected from it. Corresponding vertical ocean diffusivity values are identified using the non-linear mapping between climate sensitivity and ocean diffusivity (Urban and Keller, 2009). We use the eighteen sets of damage function coefficients obtained from experts assessment reported by Nordhaus (1994) to incorporate uncertainty in climatic damage. Finally, seven samples for the abatement cost scaling coefficient are taken from a uniform distribution centered on the value used in the DICE-07 model (Nordhaus, 2008) and covering 30 percent of this value in both directions. Thus, we generate a total of 50x18x7 = 6300 combination of parameter values representing equally likely SOW.

5.3 COMPARISON OF RESULTS WITH GTK

The modified DICE is built using our understanding of the different modifications namely, DOECLIM, Lempert's damage function and Newell and Pizer discount rates. In

order to verify our model, we begin by comparing our base case results with GTK. For the base case analysis, emission control rates reported by GTK are used in our model. We use the similar parameters settings as GTK if sufficient information was available; otherwise, values described in the literature are used.

5.3.1 Deterministic Results

Figure 5.1 presents the radiative forcing and temperature changes for BAU, optimal abatement, continuous GEO, and intermittent GEO. Our results match closely with GTK. As they highlighted, we see that once geoengineering is aborted, atmospheric temperature increases rapidly, returning after about 40 years to the level that would have been obtained under BAU. This is not surprising since the application of SRM can only reduce the amount of forcing reaching the earth's surface but does not reduce the CO_2 concentration in the atmosphere. As a result, when SRM is aborted the net radiative forcing quickly increases causing the temperature hike. This issue has, of course, been raised by several authors including Wigley (2006) and Matthews and Caldeira (2007).

Figure 5.2 presents the economic damages (climate damage and abatement costs) and abatement rate for our implementation of the GTK model. Our results again closely match with GTK. Damages increase above the BAU scenario when GEO is aborted; slightly exceeding 6% of GWP. BAU damages exceed 2% of GWP in 2075, and total damages under abatement surpass 2% of GWP around 2055.

Figure 5.1 and 5.2 also contains the DICE-07's estimates of the optimal radiative forcing, temperature change, total costs, and abatement (i.e., these values under a policy of optimal abatement). GTK's modification of DICE-07 has significantly increased climate damages and therefore the optimal level of abatement. For example, under DICE-07 the maximum temperature change reaches 3.5K, whereas GTK's model implements a level of abatement sufficient to hold temperature changes below 2K. As indicated above, we view the abatement level obtained by GTK as very high compared to DICE-07 and impractical.

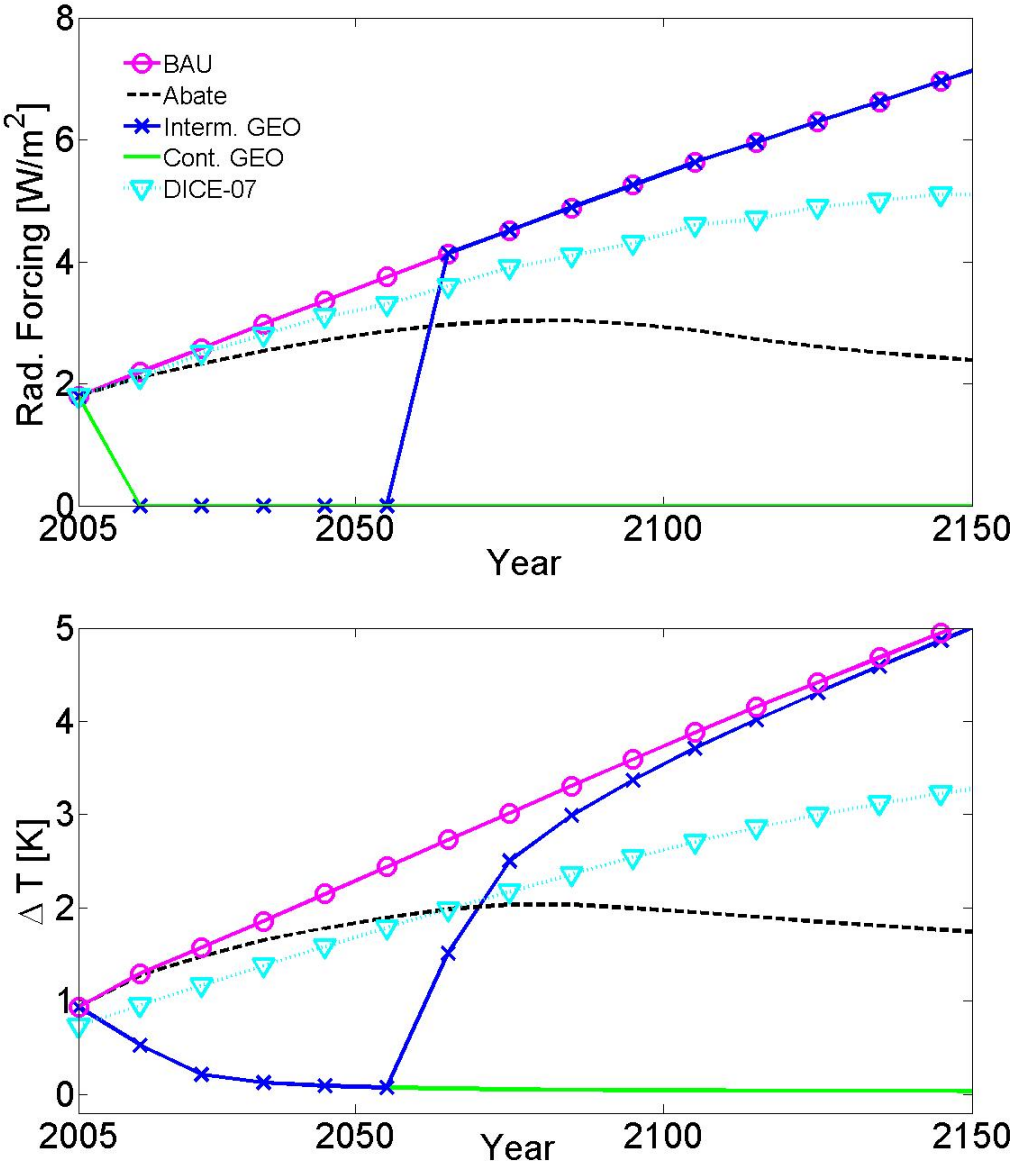

Figure 5.1 Radiative forcing (top panel), and global mean surface temperature change (bottom panel), for BAU (circles), optimal abatement (dashed line), continuous geoengineering (solid line), and intermittent geoengineering (crosses). DICE-07 results (triangles) are added as a reference. These results are based on mean inputs (not averaged over all 6300 SOW) and neglect potential economic damages due to aerosol geoengineering forcing.

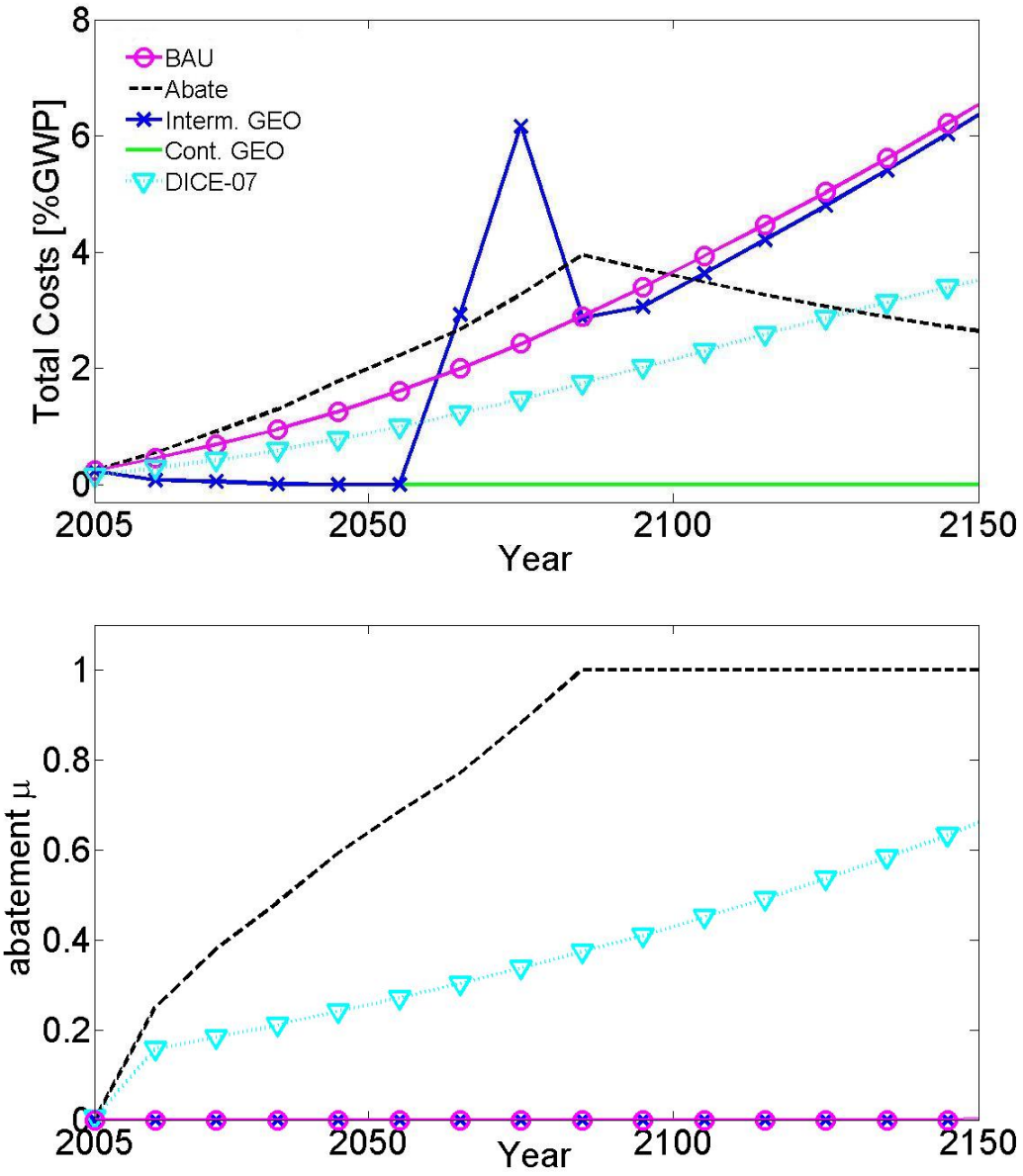

Figure 5.2 Total costs of climate change (abatement costs plus climate damages), (top panel) and fraction of CO_2 abatement (bottom panel), for BAU (circles), abatement (dashed line), intermittent geoengineering (crosses), and continuous geoengineering (solid line). DICE-07 results (triangles) are added as a reference. These results are based on mean inputs (not averaged over all 6300 SOW) and neglect potential economic damages due to aerosol geoengineering forcing.

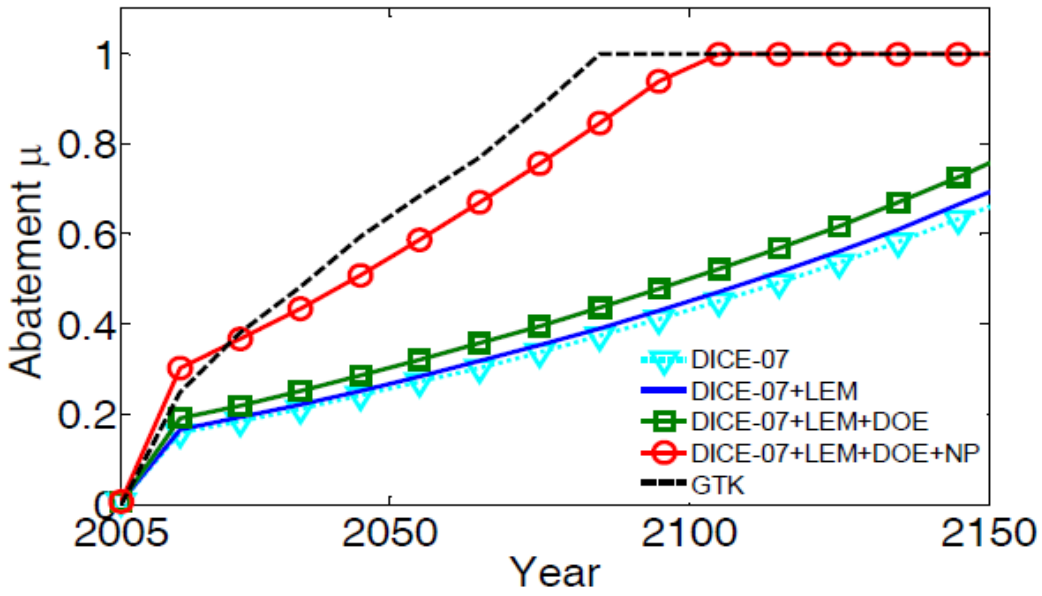

Figure 5.3 Effect of GTK modeling changes on the optimal level of emissions controls. The difference between GTK's and DICE-07's abatement strategies is dominated by GTK's change to DICE-07's discounting.

Next we compare the emission control rates induced by different modeling changes in the DICE model. The results are shown in Figure 5.3. In order to calculate the impacts made by each modification on the performance of DICE, we first study the model with only one modification at a time. Then, we analyze the model with two modifications together to incorporate the interactions between different modifications. DICE-07 + LEM represent the abatement rates obtained when DICE damage function is replaced with Lempert's. DICE-07 + LEM + DOE is the effect of replacing DICE's damage function with Lempert's and replacing DICE's climate model with DOECLIM. Finally, DICE-07 + LEM + DOE + NP is the effect of making the previous two changes and also replacing DICE-07's discounting with the Newell and Pizer methodology used by GTK. The difference between DICE-07 + LEM + DOE + NP and GTK is that the former is based on mean input values whereas the latter has been optimized under uncertainty. While there is some difference between these strategies, they are rather close. The emission control rates from DICE-07 model are also included to benchmark

the changes. We can see that the primary factor responsible for difference between DICE-07 and the GTK model, in this base case, is the change to the discounting framework. While the other modeling changes (DOECLIM and the Lempert damage function) do not produce a major difference here, they play a role in the case in which GEO is aborted.

We further analyze the impact of modifications made to the DICE model by comparing the NPV of damages and abatement (Figures 5.4-5.9). The results show that instances with modified rate function (Figures 5.5, 5.7 and 5.9) have considerably higher NPVs compared to instances with the DICE discount rate function. N&P discounts the future less aggressively compared to DICE, resulting in higher NPVs. A comparison of Figure 5.4 and Figure 5.8 shows the role played by Lempert's damage function and DOECLIM when GEO is aborted. For the Interm. GEO case, with only DOECLIM the NPV is 17.8 trillion but when DOECLIM is used with Lemperts's damage function, the NPV rises to 23.4 trillion. The figure not only shows the impact of these two modifications for Interm. GEO case but also show their interdependence to capture the damage for Interm. GEO.

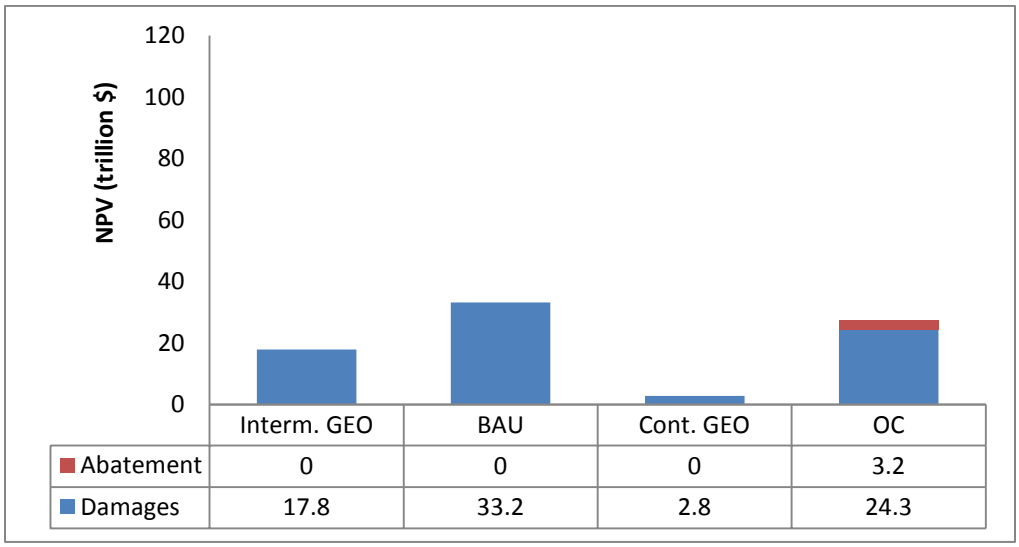

	Interm. GEO	BAU	Cont. GEO	OC
Abatement	0	0	0	3.2
Damages	17.8	33.2	2.8	24.3

Figure 5.4 NPV of damages and abatement under different policies for DICE-07 model with only DOECLIM modification.

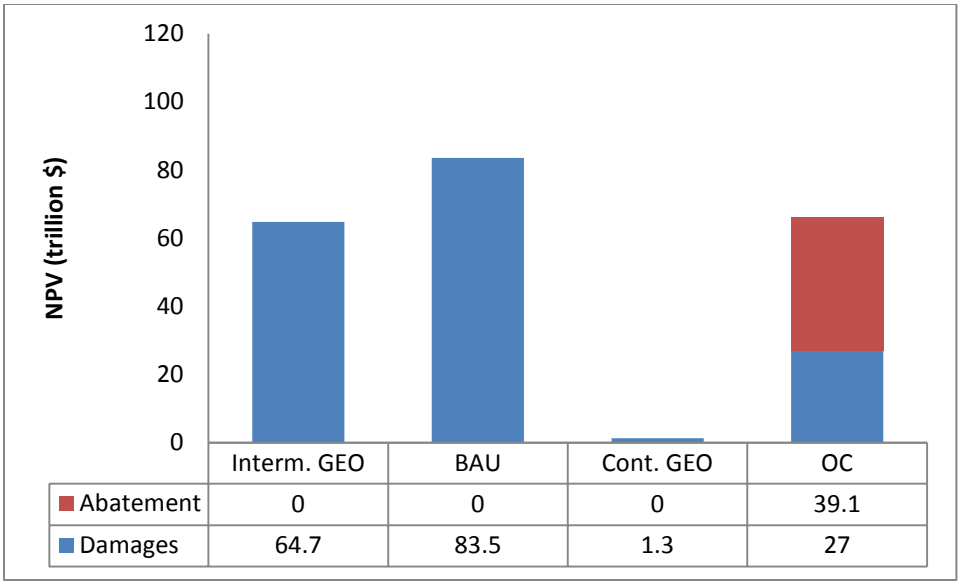

Figure 5.5 NPV of damages and abatement under different policies for DICE-07 model with only discount rate modification.

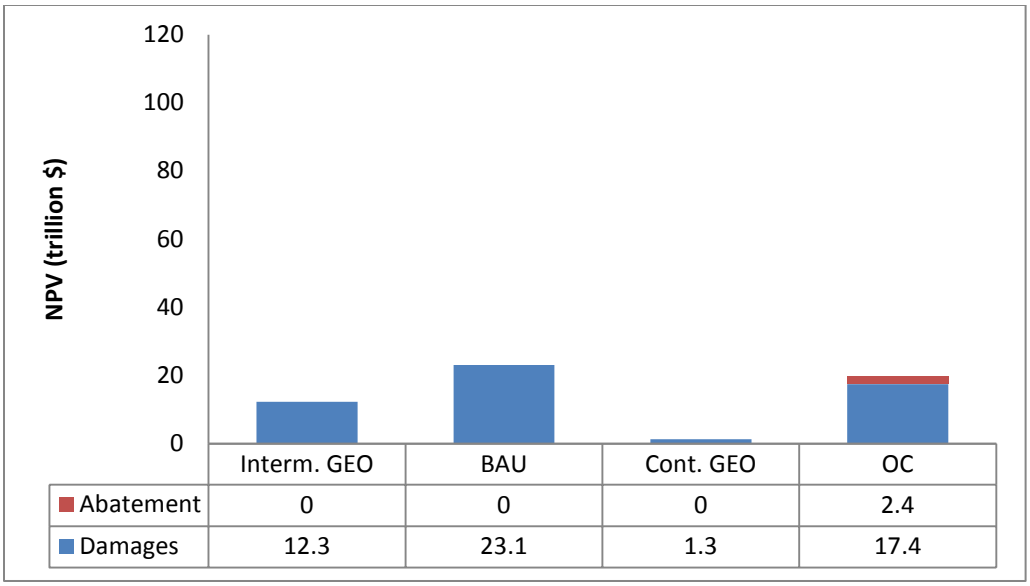

Figure 5.6 NPV of damages and abatement under different policies for DICE-07 model with only damage function modification.

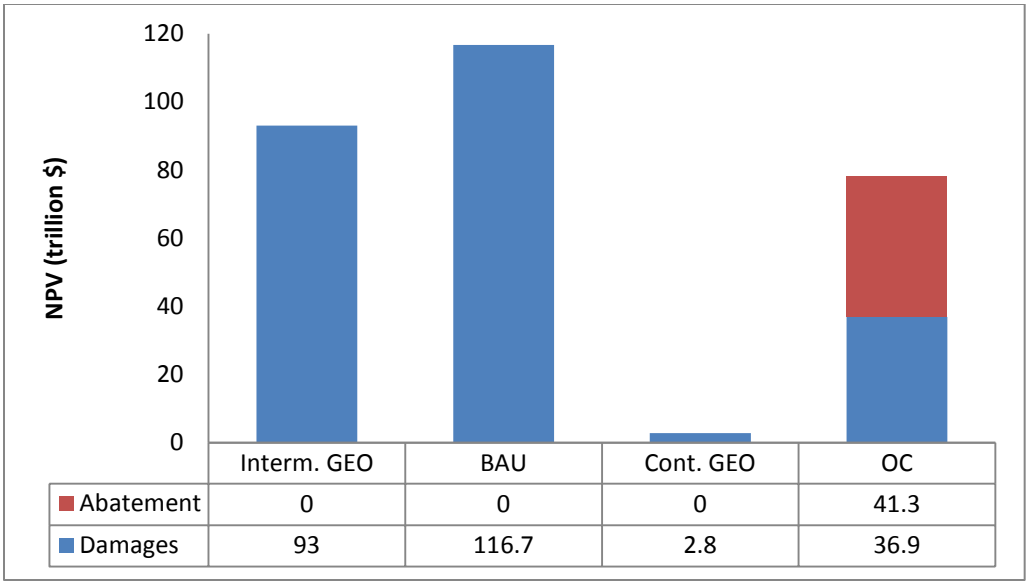

Figure 5.7 NPV of damages and abatement under different policies for DICE-07 model with DOECLIM and discount rate modification.

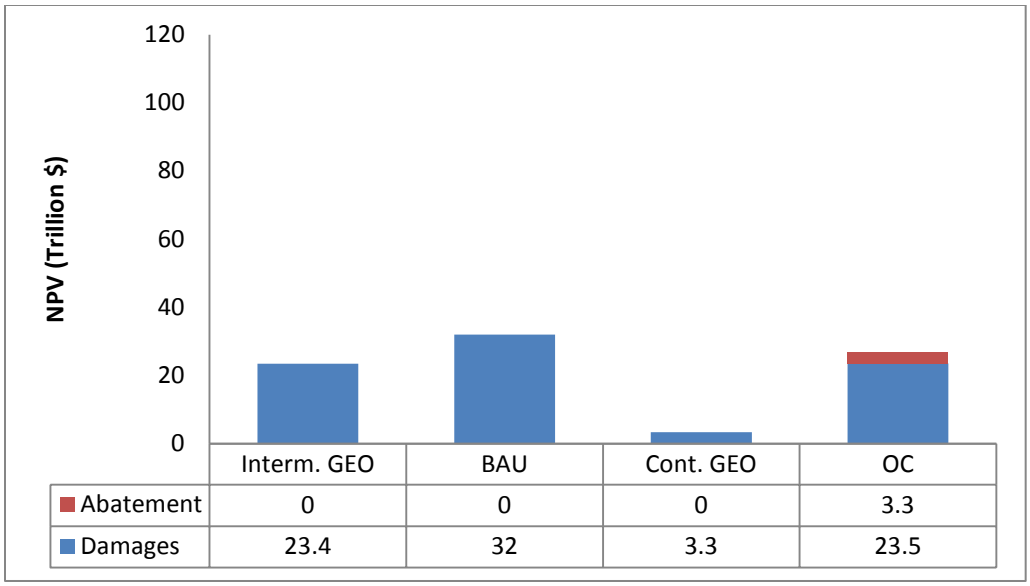

Figure 5.8 NPV of damages and abatement under different policies for DICE-07 model with DOECLIM and damage function modification.

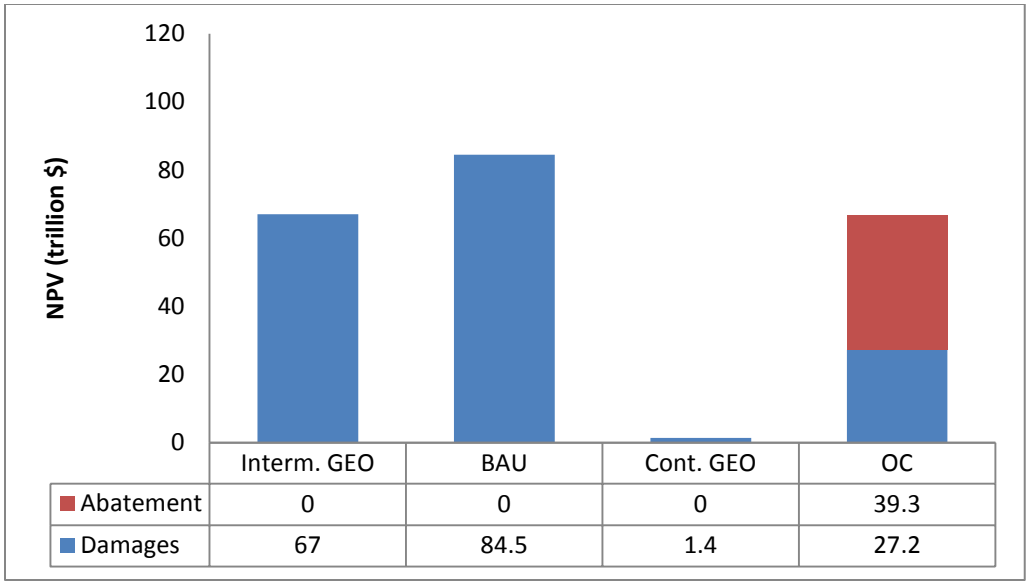

Figure 5.9 NPV of damages and abatement under different policies for DICE-07 model with discount rate and damage function modification.

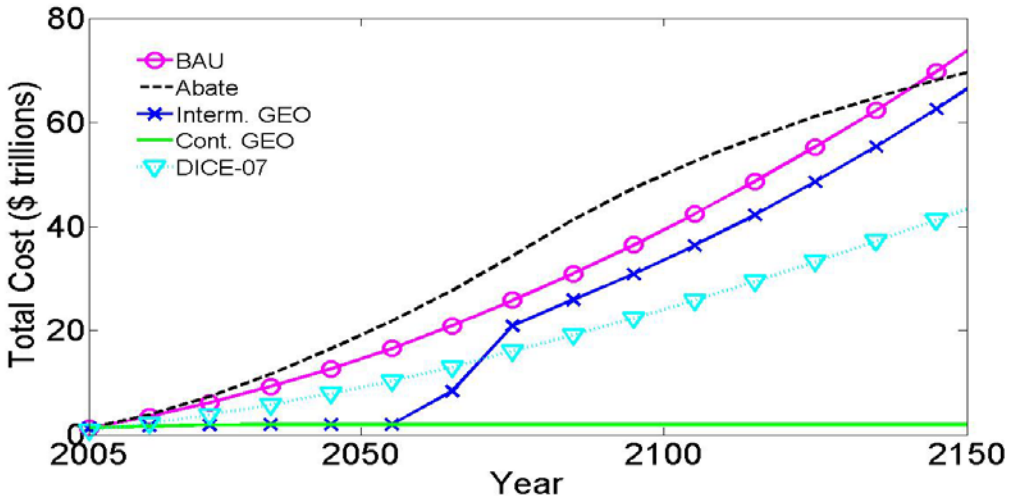

Figure 5.10 Cumulative discounted total costs of climate change (abatement costs plus climate damages) for BAU (circles), abatement (dashed line), intermittent geoengineering (crosses), and continuous geoengineering (solid line). These results are based on best-guess inputs (not averaged over all 6300 SOW) and neglect potential economic damages due to aerosol geoengineering forcing. Cumulative damages under an aborted GEO strategy are lower than BAU and optimal abatement (through 2150).

5.3.2 Probabilistic Results

The decision tree representing GTK's framing of the problem is shown in Figure 5.11. GTK considered two decision alternatives: Optimal emission control or BAU with geoengineering (BAU_GEO). They assumed that optimal control will continue forever while they associated a probability '*p*' of turning off SRM. The expected utility of decision alternatives is then calculated as (Bickel and Agrawal, 2011):

$$\mathrm{EU}[\mathrm{Alternative}, \theta] = \sum_{i=1}^{6300} \frac{1}{6300} U(SOW_i, Alternative, \theta),$$

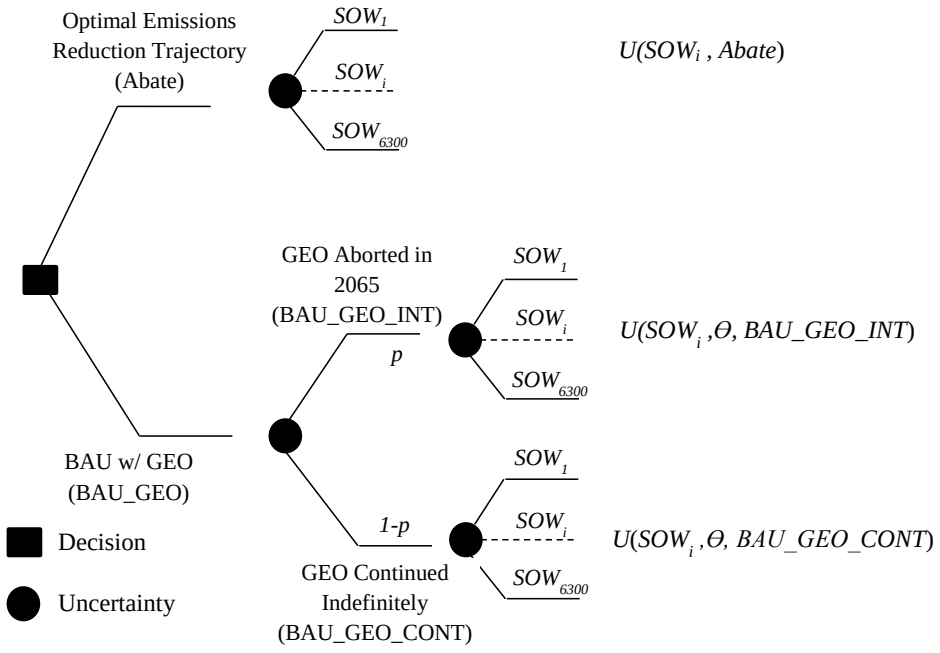

Figure 5.11 Schematic decision tree detailing GTK's framing of the aerosol geoengineering deployment decision.

where, SOW_i is the i^{th} SOW and *U* is the utility assigned to each SOW under a given decision alternative; θ is the damage caused by geoengineering (assumed zero for abatement) and measured as percentage of GWP per doubling of CO_2 radiative forcing.

The breakeven probability which will make society indifferent between optimal controls and BAU with geoengineering is then calculated as:

$$p^*(\theta) = \frac{EU\left[BAU_{GEO_{CONT}}, \theta\right] - EU[Abate]}{EU\left[BAU_{GEO_{CONT}}, \theta\right] - EU\left[BAU_{GEO_{INT}}, \theta\right]},$$

The breakeven analysis under GTK assumption is shown in Figure 5.12. The results are a close match to GTK's result. If $p^* = 0$ (GEO will be continuous), then any level of GEO damages above about 0.75% of GWP would result in optimal abatement being preferred to BAU with GEO. An increase in the probability of aborting GEO decreases the value of θ or level of damage at which breakeven will be achieved. Figure 5.12 (a) shows that GEO is not preferred for any level of damages if the probability of GEO being aborted is greater than about 0.15. The green region in the figure indicates all the probability and damage coefficient combinations at which the expected utility of BAU_GEO is greater than OC. The red region indicates all the probability and damage coefficient combinations at which the expected utility of BAU_GEO is less than OC. Thus, the green region represents the combinations at which geoengineering 'passes' a cost-benefit test while red represent the region it 'fails' the cost-benefit test.

Figure 5.12 (b) shows the same breakeven analysis but under DICE discounting. The breakeven curve obtained under GTK assumption is shown as dashed line in the figure. The figure clearly shows the considerable increase in the green region compared to Figure 5.12 (a). If the damages due to geoengineering are assumed to be 0, then the figure suggests that it's always profitable to use geoengineering (even with a 100% chance of shutdown) with no emission controls over abatement. As stated earlier, this figure again shows the importance of the discounting model used in making such decisions.

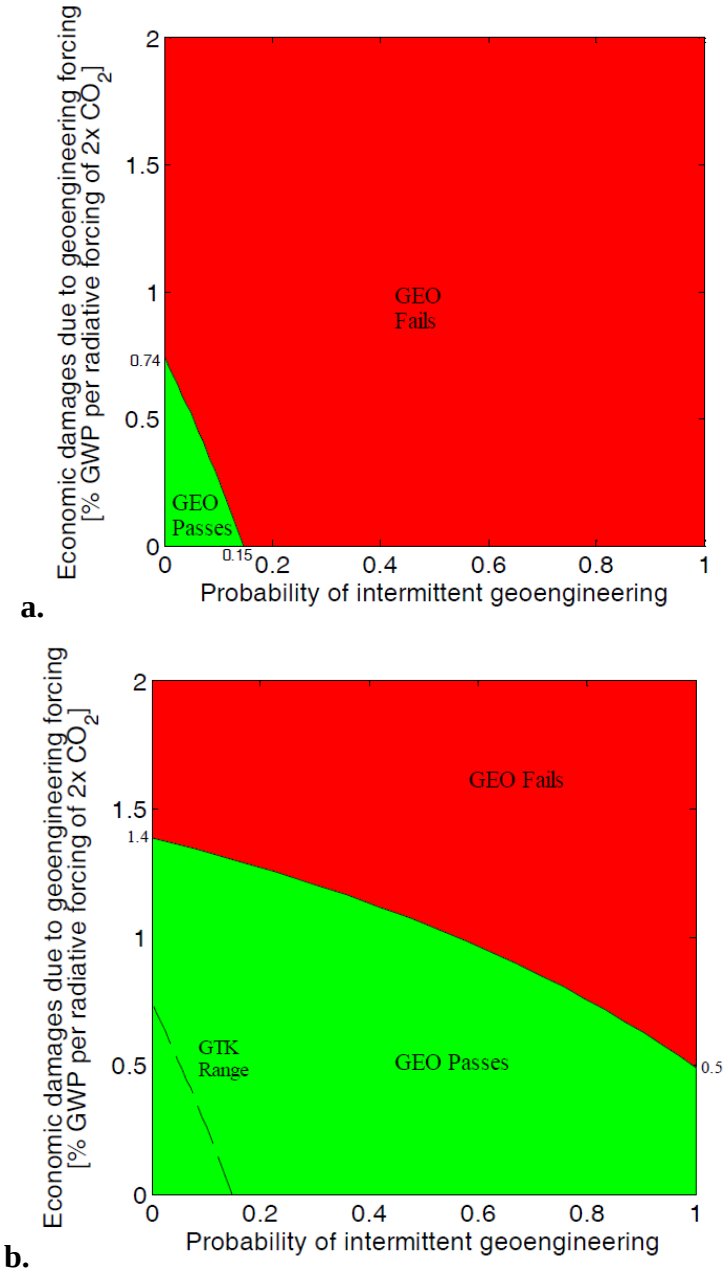

Figure 5.12 Scenario map for the cost-benefit test to substitute geoengineering for CO_2 abatement as a function of the probability of aborted geoengineering and the estimated damages due to geoengineering radiative forcing under (a) GTK discounting and (b) DICE discounting.

5.4 Extending the Analysis: Reframing the Decision Problem

GTK failed to consider society's response to an aborted geoengineering program. In addition, they always considered SRM as a replacement for emission control policy and did not investigate the benefits of a policy involving SRM with abatement. In this section, we investigate different and what we regard as more reasonable decision scenarios for thorough risk analysis of geoengineering implementation.

5.4.1 Practical Modifications to GTK's Framing

In this section we make two very practical modifications to GTK framing and evaluate the outcomes under GTK and DICE discounting. First, we investigate the scenario where society responds after turning off GEO by initiating an optimal control policy. Second, we explore the case when optimal control could also be turned off with a similar probability as GEO.

5.4.1.1 Intermittent SRM with Abatement after Shutdown

In this scenario we have assumed that society responds by implementing an optimal control policy after the SRM is aborted. This case is similar to GTK except that under intermittent SRM, emission control is deployed after shutdown instead of a BAU policy. The decision tree for this scenario is shown in Figure 5.13. In this scenario, after the SRM is aborted with probability *p*, society chooses to adopt GTK's emission control policy beginning in year 2065 (i.e., shift the start date to 2065 but do not optimize for emission control rates). We do not claim that this response is optimal. Rather, we are simply providing a framework that we believe is (minimally) consistent with GTK's assumption that the choice is between BAU and optimal abatement.

The scenario maps obtained under the aforementioned decision framework using GTK and DICE discounting are shown in Figure 5.14(a) and 5.14(b) respectively. The breakeven line obtained by GTK is also included in both the figures as dotted black line. The results show that incorporating the ability to respond to an aborted GEO program

significantly increases the green region of the scenario maps. The threshold at which GEO fails a cost-benefit test when damage due to GEO forcing is zero has increased from 0.15 to 0.89 under GTK discounting. Under DICE discounting, the θ value at which BAU_GEO with any probability of aborting breakeven with OC is increased from 0.5 to 0.9%.

5.4.1.2 Intermittent Emission Controls

GTK assumed a continuous emission control scenario. We argue that if GEO can be aborted then why not abatement? We do not see any reason this assumption must hold and analyzed the scenario where emission control and geoengineering both can be aborted with same probability *p*. In the case of an aborted program of emissions controls, we assume that emissions controls are phased out as installed capital stock is retired. As an illustrative example, we assume that emissions reductions decrease linearly from their 2055 level to 0% over 40 years.

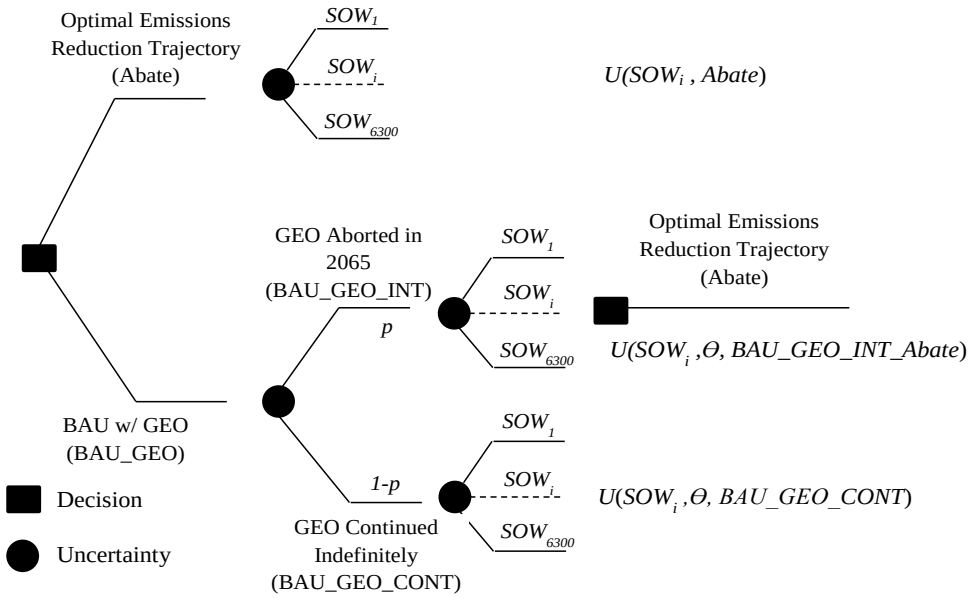

Figure 5.13 Decision tree for decision scenario that allows society to respond to an aborted GEO program by implementing abatement.

Figure 5.15(a) and (b) present the scenario maps for this case under GTK and DICE discounting, respectively. The figure again shows a considerable increase in the acceptable region compared to GTK. The figure suggests that under GTK discounting, when damage due to GEO forcing is zero, GEO is always profitable. Under DICE discounting, the θ value at which BAU_GEO with any probability of aborting breakeven with OC is increased from 0.5 to 0.86%.

5.4.2 BAU and Abatement with Geoengineering

As we have stated earlier, geoengineering is not an 'OR' alternative but it is an 'AND' strategy, which can be coupled with other strategies to maximize the benefits and reduce risks. Thus a reasonable analysis of the benefits and risk of geoengineering should be done considering it as an incremental strategy. In this section we demonstrate the benefits of using geoengineering with BAU and abatement, respectively.

5.4.2.1 GEO with BAU

In this scenario, we consider the problem where society faces a decision between no emission controls or BAU and BAU_GEO. The decision tree structure for this problem is shown in Figure 5.16. The scenario maps for this case are shown in Figure 5.17(a) and 5.17(b) for GTK and DICE discounting, respectively.

The figure shows that GEO passes the cost benefit taste for almost the entire region under GTK discounting. In previous scenarios, the use of DICE discounting always lead to a significant increase in the acceptable region. However, the acceptable region for DICE discounting is comparatively smaller than GTK discounting in this case. This is because high values of θ (greater than the damages under BAU) impose a cost in the near term for the possibility of a future benefit (if GEO is not aborted). These future benefits are not valued as highly under DICE discounting. Thus, changing the discount rate can make GEO more or less attractive.

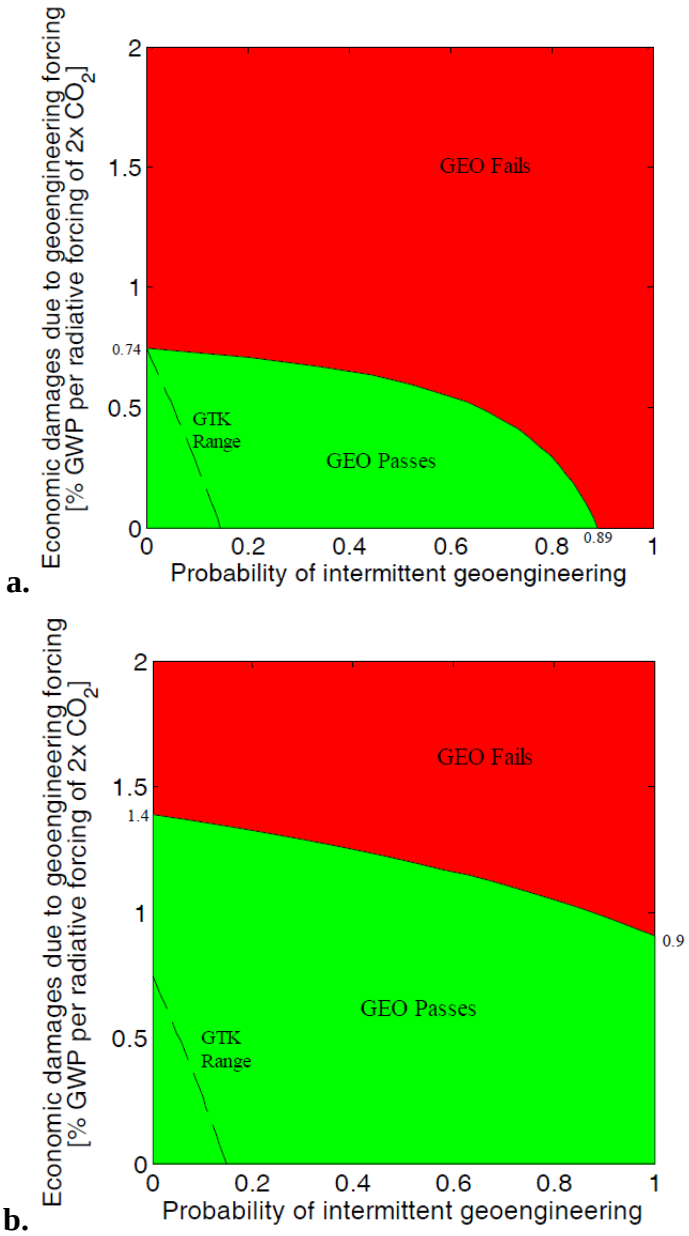

Figure 5.14 Scenario map for the cost-benefit test to substitute geoengineering for CO_2 abatement, including the option to implement emissions reductions if the geoengineering program is aborted, as a function of the probability of aborted geoengineering and the estimated damages due to geoengineering radiative forcing under GTK discounting (panel a) or DICE discounting (panel b).

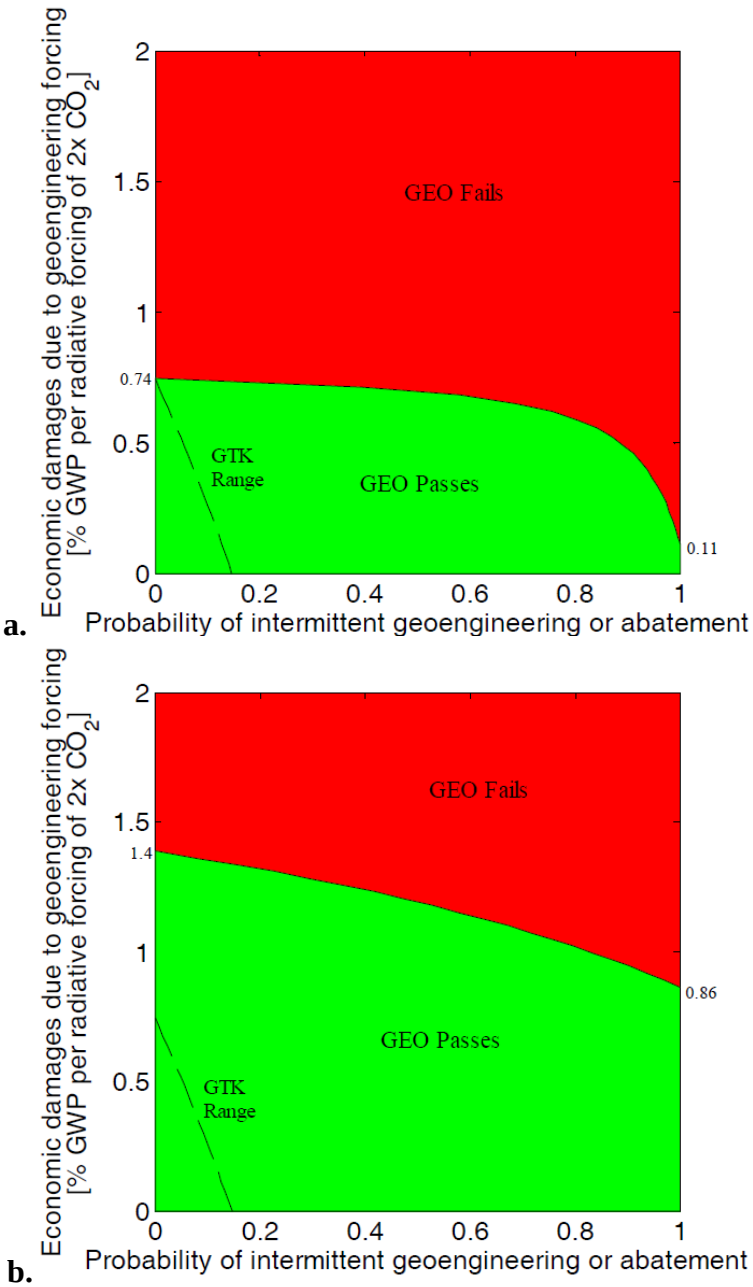

Figure 5.15 Scenario map for the cost-benefit test to substitute geoengineering for CO_2 abatement, assuming that both geoengineering and emissions controls could be aborted under GTK discounting (panel a) or DICE discounting (panel b).

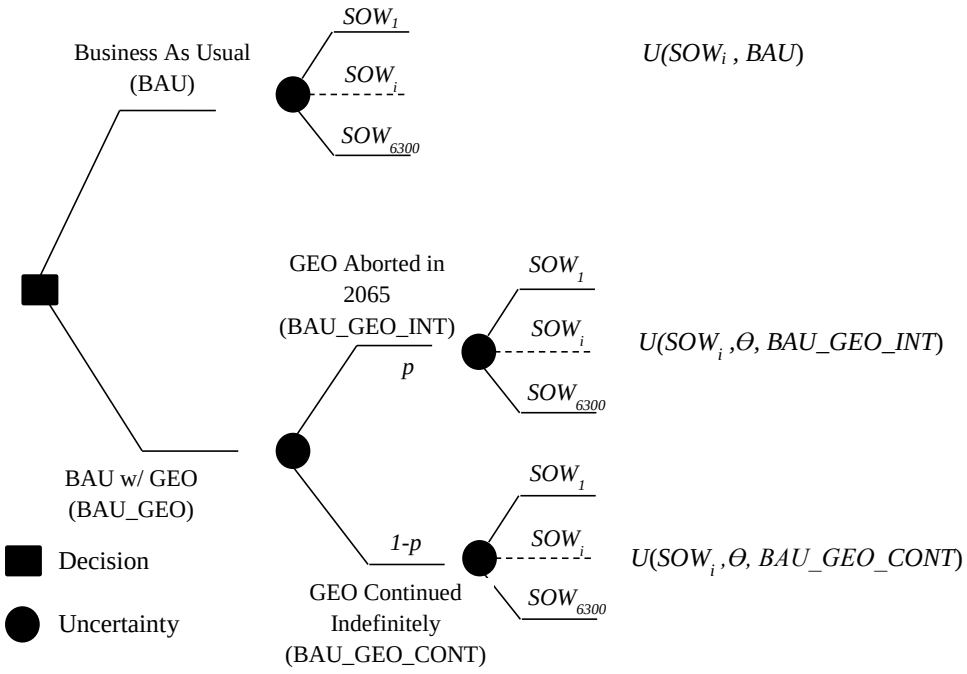

Figure 5.16 Decision tree for decision scenario that allows society to choose between GEO and BAU.

5.4.2.2 GEO with Abatement

Several authors (Wigley 2006; Bickel and Lane 2010) have suggested that the use of geoengineering in conjunction with emissions controls may present an economical and possibly less risky strategy than pursuing emissions reductions alone. GEO can be used to rapidly stabilize temperature while abatement can be used to slowly decrease carbon concentration in the atmosphere. In order to test this strategy, we assume that society agrees to adopt a GEO strategy where 1 W m^{-2} of negative forcing is provided via aerosol injection (GEO1).

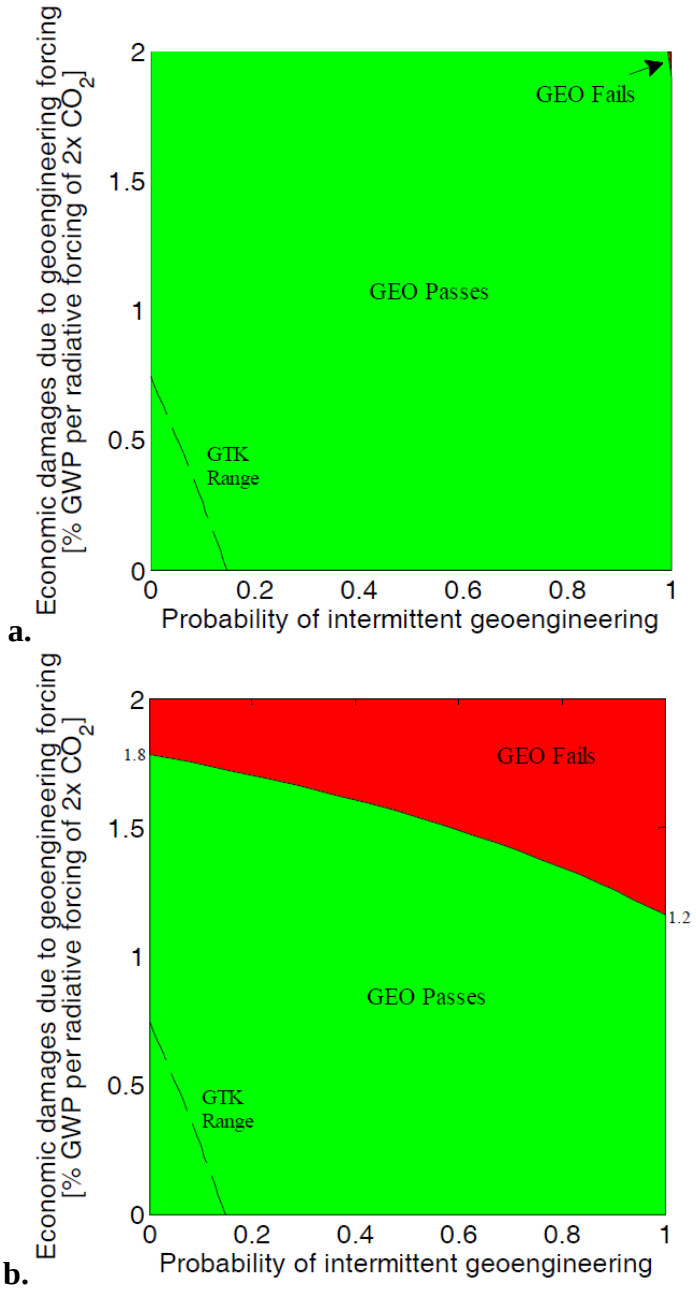

Figure 5.17 Scenario map for the cost-benefit test to add geoengineering to a BAU policy under GTK discounting (panel a) or DICE discounting (panel b). Geoengineering now passes the cost-benefit test for almost the entire range of values tested by GTK (panel a). Viewing GEO as an incremental policy change greatly enlarges the region in which is passes a cost-benefit test, compared to GTK's conclusions.

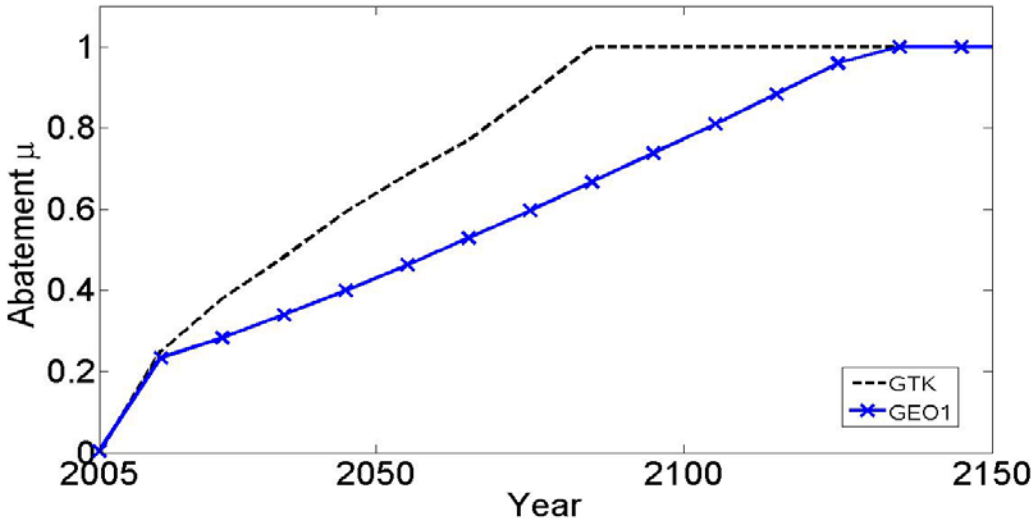

Figure 5.18 Emission control profile under GEO1 and GTK.

Based on the knowledge that GEO1 will be implemented, society chooses an emissions trajectory, which will be lower than the one that would be selected under a policy of emissions controls without GEO. We further assume that society chooses this emissions control strategy under the belief, perhaps mistaken, that its GEO1 program will be in place indefinitely. We found this level of emissions reductions by assuming mean values for the parametric uncertainties. The emission trajectory under GEO1 is obtained using GAMS model of DICE with GTK modifications. GEO1 should simply be viewed as a possible emissions control strategy (Figure 5.18). In this case, we again assume that if GEO1 is aborted, then society cannot increase its abatement. Relaxing this assumption or computing the optimal emissions control profile would only strengthen our results, which are presented in Fig. 5.19. The results show that GEO1 with abatement again passes the cost benefit test over most of the scenarios considered by GTK. Use of DICE discounting further seem to increase the acceptable region of the curve.

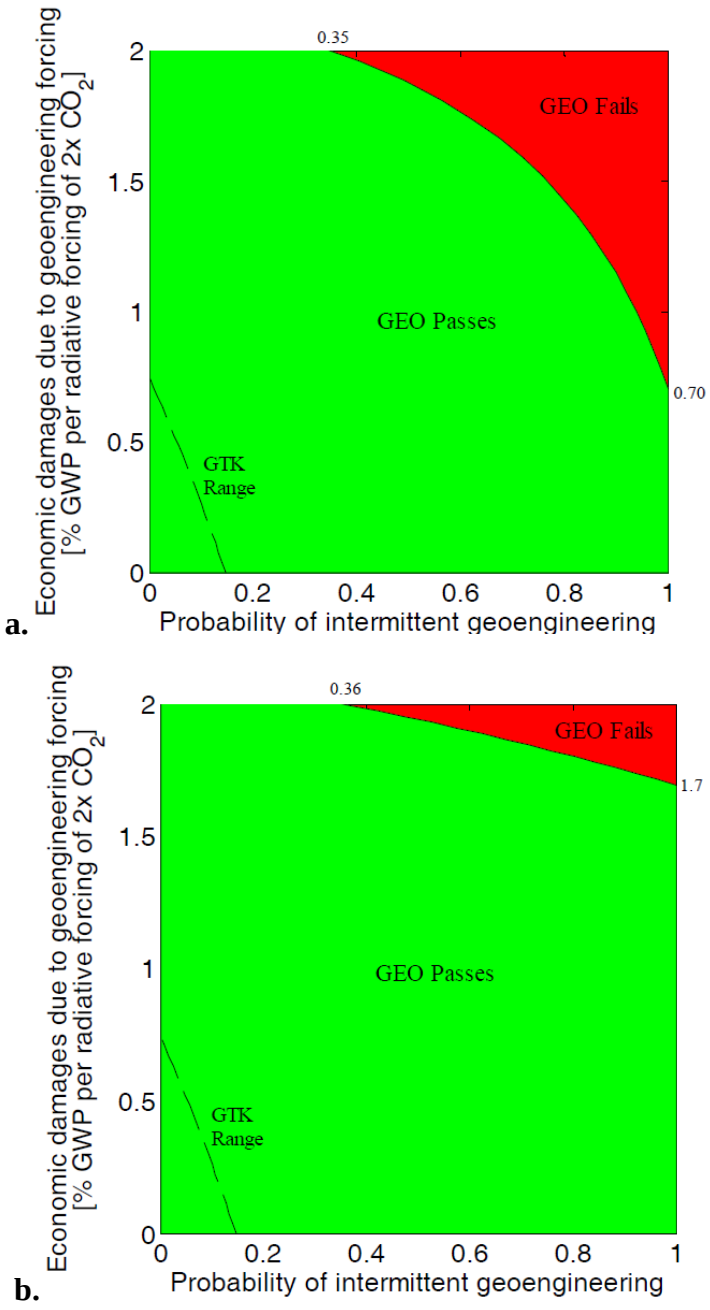

Figure 5.19 Scenario map for the cost-benefit test to add geoengineering to a policy emissions reductions under GTK discounting (panel a) or DICE discounting (panel b). Geoengineering now passes the cost-benefit test over a wide range of values tested by GTK.

Chapter 6 Application in Financial Sector

Risk management is considered a challenging problem in financial sector and different tools and techniques have been developed over time to mitigate risk. In the financial services industry, risk is divided into three categories (Schuermann, 1997):

1. **Market Risk:** Market risk induced by the changes in market condition, for example, losses due to decrease in market value of a commodity, and comes from different sources including: interest rate fluctuations, foreign exchange fluctuations, supply/demand fluctuation and change in volatility of interest rates.
2. **Credit Risk:** Credit risk entails the losses incurred due to non-payment by the counterparty in the financial transaction. Examples of this type of risk are credit card defaults, loan defaults, etc.
3. **Operating Risk:** Operating risk covers all the residual sources of risk after taking into account market and credit risk. It is the risk associated with daily operating of the business and include: system failures, fraud, litigation, settlement failure, errors and omissions.

Most financial firms have strategies in place to manage market risk. Long term contracts, well-diversified portfolios, insurance and financial derivatives are some of the tools to manage market risk effectively. Financial firms strive to mitigate credit risk (by doing business with ‘good’ customers) failing which the focus shifts to its early detection. Risk detection is treated as a statistical problem in the financial sector, where risk is defined as potential for deviation from expected results. Credit risk is detected using sophisticated statistical models which utilize huge data sets available with the company or obtained from credit bureaus and essentially compare the observed data with the expected value (Bolton and Hand, 2002). The statistical analysis returns a ‘score’ which measures the creditworthiness of the counterparties involved (in general, a higher score is regarded as more creditworthy than a lower one). Similar statistical models are in use for fraud detection where the model outputs ‘suspicion score’. A higher suspicion score

indicates unusual and potentially fraudulent transactions. These scores are updated regularly, rank ordered and stored in database. Accounts with unusual scores are further analyzed for credit or fraud risk detection purposes.

The models for credit risk detection in financial industry can be categorized as: supervised and unsupervised. Supervised models use data from previous types of fraud and non-fraudulent records to construct the model. Pattern recognition and data mining tools are used to build such models. A new observation is placed into one of these categories which it resembles most. This model requires availability of large amount of data and can only detect risks which are previously encountered. Unsupervised models are built when the data is not available for fraud and legitimate transactions. It uses profiling and outlier detection method to identify customers which are most dissimilar from the rest of the group. Normal behavior is modeled by a baseline distribution and observations that show greatest detection from this norm are identified. For example, PayPal uses an Explosive Growth model which is based on increase in total purchasing volume (TPV) and flags a customer if the ratio of current TPV and previous TPV increases above a pre-defined threshold. The flagged accounts then go for primary review where an agent reviews them for riskiness based upon the available information. If the agent finds an account as suspicious, he/she then forwards it for ‘deep dive’ where more information is gathered for the account. Once an account is identified as bad, appropriate actions (warnings, holds and restriction) are taken to minimize the risk.

The construction of a risk and fraud detection model is very challenging and needs continuous improvement because fraudsters adapt their strategies to circumvent detection. The exchange of knowledge between different companies is very limited making risk and fraud difficult to assess. Another problem encountered with risk or fraud detection is the magnitude of fair transactions for each fraudulent one. In general, 1 out of every 1000 transactions is fraudulent (Bolton and Hand, 2002). A 99% accurate detection method which can be considered highly effective, will still predict 10 transactions as fraudulent. Separating 9 legitimate transactions from the 10 predicted as suspicious can

involve considerable cost. Risk managers, now, are challenged to develop statistical models that keep per unit processing cost low and satisfactorily assess credit or fraud risk. In spite of all these limitations, risk detection is an important part of any financial institution. It not only prevents the direct losses through fraudulent transactions but also strengthens consumer trust in the company thereby preventing revenue loss from lost sales.

Chapter 7 Conclusion

In this thesis, we have demonstrated the application of decision analysis and risk management tools to solve problems associated with climate change and risk detection. Tools like decision trees, scenario analysis and statistical modeling were used to show their effectiveness in practical problems, which require complex decision making and risk mitigation.

The climate change problem we considered involved evaluating geoengineering as a viable option to mitigate climate change risk. Earlier GTK argued that geoengineering is not a viable option if there is a positive probability of it aborting. From all the analysis we have conducted, it is clear that GTK's conclusion is based on their framing of the problem. Using similar scenarios but with new framing of the problem, which seems more rational, reasonable and practical, we showed that geoengineering in fact passes the cost benefit test for a wide range of scenarios. This example brilliantly shows that how framing of decision problem can lead to totally different conclusions. A decision maker should exercise caution while framing the problem to avoid ending up with wrong decision. We have also investigated the relative importance of different modifications made to DICE model and conclude that discounting has the biggest impact on results. With DICE discounting, which is argued to be correct by Goliath and Weitzman (2010), the region where geoengineering passes the cost-benefit test is larger than under a discounting method proposed by Newell and Pizer (2004).

We have also explained how risk detection is an important part of risk management in the financial services industry. The industry faces three main types of risk: market risk, credit risk and operational risk. The detection and prevention of credit risk due to fraud is most challenging and important as it affects the company in the long run. Statistical models used by the industry to detect and prevent these types of risk can be categorized into supervised and unsupervised. The thesis provides an overview of these models and their limitations.

References

Bickel J.E., and Agrawal S., 2011, Reexamining the economics of aerosol geoengineering, in review at Climatic Change, pp. 1-26.

Bickel J.E., and Lane L. 2010, Climate engineering. In: Lomborg B (ed) Smart responses to climate change: Comparing costs and benefits, Cambridge University Press, Cambridge, UK, pp. 9–51.

Bolton R.J., and Hand D.J., 2002, Statistical fraud detection: A review, Statistical Science, 17(3), pp. 235–255.

Crutzen P.J., 2006, Albedo enhancement by stratospheric sulfur injections: A contribution to resolve a policy dilemma?, Climatic Change, 77(3-4), pp. 211-220.

Goes M., Tuana N., and Keller K., 2011, The economics (or lack thereof) of aerosol geoengineering, Climatic Change, DOI: 10.1007/s10584-010-9961-z

Gollier C., 2009, Should we discount the far-distant future at its lowest possible rate? Economics: The Open-Access, Open-Assessment E-Journal 3(2009-25) DOI: 10.5018/economicsejournal.ja.2009-5025, http://dx.doi.org/5010.5018/economics-ejournal.ja.2009-5025ja.2009-5025.

Gollier C., and Weitzman M.L., 2010, How should the distant future be discounted when discount rates are uncertain? Economics Letters 107, pp. 350–353.

Intergovernmental Panel on Climate Change, 2007, Climate change 2007: Mitigation, B. Metz, O. Davidson, P. Bosch, R. Dave, and L. Meyer (eds), Cambridge University Press, New York, NY.

Kriegler E., 2005, Imprecise probability analysis for integrated assessment of climate change. Dissertation, University of Potsdam.

Lempert R.J., Schlesinger M.E., and Bankes S.C., 2000, The impacts of climate variability on near term policy choices and the value of information, Climatic Change 45, pp. 129–161.

Lenton T.M., Held H., and Kriegler E., 2008, Tipping elements in the earth's climate system, PNAS 105(6), pp. 1786–1793.

Matthews H.D., and Caldeira K., 2007, Transient climate-carbon simulations of planetary geoengineering, PNAS 104(24), pp. 9949–9954.

Newell R.G., and Pizer W.A., 2004, Uncertain discount rates in climate policy analysis, Energy Policy, 32, pp. 519–529.

Nordhaus W.D., 1994, Expert opinion on climatic change, American Scientist, 82, pp. 45-51.

Nordhaus W.D., 2008, A question of balance, Yale University Press, New Haven.

Royal Society (prepared by J. Shepherd et al.), 2009, Geoengineering the climate: Science, governance and uncertainty, London: Science Policy Centre of The Royal Society, pp. 1-98.

Schneider von Deimling, Held T.H., Ganopolski A., and Rahmstorf S., 2006, Climate sensitivity range derived from large ensemble simulations of glacial climate constrained by proxy data, Climate Dynamics, 27, pp. 149–163.

Schuermann, T., 1997, Risk Management In The Financial Services Industry: Through A Statistical Lens, AAAI Technical Report WS-97-07.

Urban, N.M., and Keller, K., 2009, Complementary observational constraints on climate sensitivity, Geophysical Research Letters, 36, pp. 1-4.

Wigley T.M.L., 2006, A combined mitigation/geoengineering approach to climate stabilization, Science, 314(5798), pp. 452-454.